BTN2A1, an immune checkpoint targeting Vγ9Vδ2 T cell cytotoxicity against malignant cells

Carla Cano, Christine Pasero, Aude de Gassart, Clement Kerneur, Mélanie Gabriac, Marie Fullana, Emilie Granarolo, René Hoet, Emmanuel Scotet, Chirine Rafia, et al.

Cell Reports

Article

BTN2A1, an immune checkpoint targeting Vγ9Vδ2 T cell cytotoxicity against malignant cells

Graphical abstract

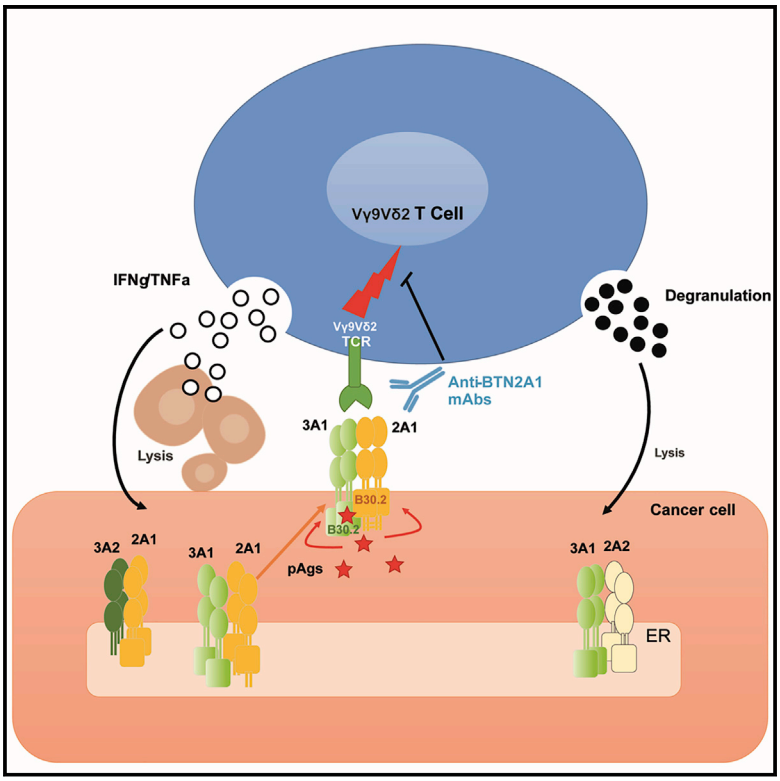

Highlights

- BTN2A1 expression in cancer cells correlates with Vγ9Vδ2 T cell cytotoxicity
- BTN2A1 interacts with BTN3A1/3A2/3A3, leading to enhanced plasma membrane export
- B30.2 domains of both BTN3A1 and BTN2A1 are required for pAg responsiveness
- Anti-BTN2A1 mAbs blocking Vγ9Vδ2TCR binding antagonize Vγ9Vδ2 T cell cytotoxicity

Authors

Carla E. Cano, Christine Pasero, Aude De Gassart, ..., Antoine Briantais, Anne Charlotte le Floch, Daniel Olive

Correspondence

carla.cano@imcheck.fr (C.E.C.), daniel.olive@inserm.fr (D.O.)

In brief

Cano et al. show that targeting BTN2A1 with mAbs allows modulation of Vγ9Vδ2 T cell cytotoxicity against primary cancer cells. BTN2A1 expression correlates with antitumoral Vγ9Vδ2 T cell responses. BTN2A1 export at the plasma membrane is strongly enhanced by interaction with BTN3A1, and this interaction is enhanced by amino-biphosphonate treatment.

Cano et al., 2021, Cell Reports *36*, 109359
July 13, 2021
https://doi.org/10.1016/j.celrep.2021.109359

CellPress

Cell Reports

CellPress
OPEN ACCESS

Article

BTN2A1, an immune checkpoint targeting Vγ9Vδ2 T cell cytotoxicity against malignant cells

Carla E. Cano,[1,8,*] Christine Pasero,[1] Aude De Gassart,[1] Clement Kerneur,[1] Mélanie Gabriac,[1] Marie Fullana,[1] Emilie Granarolo,[1] René Hoet,[1] Emmanuel Scotet,[2,3] Chirine Rafia,[1,2,3] Thomas Herrmann,[4] Caroline Imbert,[5] Laurent Gorvel,[5] Norbert Vey,[6] Antoine Briantais,[5] Anne Charlotte le Floch,[5] and Daniel Olive[5,6,7,*]

[1]ImCheck Therapeutics, 31 Joseph Aiguier, 13009 Marseille, France
[2]Université de Nantes, INSERM, CNRS, CRCINA, 44000 Nantes, France
[3]LabEx IGO "Immunotherapy, Graft, Oncology," Nantes 44000, France
[4]Institute for Virology and Immunobiology, University of Würzburg, 97078 Würzburg, Germany
[5]Centre de Recherche en Cancérologie de Marseille (CRCM), INSERM U1068, 13009 Marseille, France
[6]Institut Paoli-Calmettes, 13009 Marseille, France
[7]Aix-Marseille Université UM105, CNRS UMR 7258, 13009 Marseille, France
[8]Lead contact
*Correspondence: carla.cano@imcheck.fr (C.E.C.), daniel.olive@inserm.fr (D.O.)
https://doi.org/10.1016/j.celrep.2021.109359

SUMMARY

The anti-tumor response of Vγ9Vδ2 T cells requires the sensing of accumulated phosphoantigens (pAgs) bound intracellularly to butyrophilin 3A1 (BTN3A1). In this study, we show that butyrophilin 2A1 (BTN2A1) is required for BTN3A-mediated Vγ9Vδ2 T cell cytotoxicity against cancer cells, and that expression of the BTN2A1/BTN3A1 complex is sufficient to trigger Vγ9Vδ2 TCR activation. Also, BTN2A1 interacts with all isoforms of BTN3A (BTN3A1, BTN3A2, BTN3A3), which appears to be a rate-limiting factor to BTN2A1 export to the plasma membrane. BTN2A1/BTN3A1 interaction is enhanced by pAgs and, strikingly, B30.2 domains of both proteins are required for pAg responsiveness. BTN2A1 expression in cancer cells correlates with bisphosphonate-induced Vγ9Vδ2 T cell cytotoxicity. Vγ9Vδ2 T cell killing of cancer cells is modulated by anti-BTN2A1 monoclonal antibodies (mAbs), whose action relies on the inhibition of BTN2A1 binding to the Vγ9Vδ2TCR. This demonstrates the potential of BTN2A1 as a therapeutic target and adds to the emerging butyrophilin-family cooperation pathway in γδ T cell activation.

INTRODUCTION

Unraveling the essential components of γδ T cell-mediated antitumor responses is critical for understanding γδ T cells and their use as novel therapies. Unlike conventional αβ T cells, which carry TCRs encoded by the *TRA* and *TRB* gene loci, γδ T cells do not require antigen presentation by the major histocompatibility complex (MHC). Instead, they respond to a variety of stimuli binding directly to their TCR, whose reactivities are determined by the different *TRG* and *TRD* gene loci used to produce the TCR (Adams et al., 2015). The predominant γδ T cells in the peripheral blood are Vγ9Vδ2 T cells. These cells represent 1%–10% of circulating T cells in healthy individuals, and they are activated by intracellular phosphoantigens (pAgs) from malignant or bacterial origins (Morita et al., 2007). pAgs are pyrophosphorylated intermediates from the isoprenoid mevalonate and non-mevalonate biosynthetic pathways found in vertebrates and bacteria, respectively (Heuston et al., 2012; Tanaka et al., 1995). Both pathways produce distinct pAg intermediates, which differ in their ability to stimulate Vγ9Vδ2 T cells; for example, (*E*)-4-hydroxy-3-methyl-but-2-enyl diphosphate (HMBPP) from the bacterial pathway is 10,000-fold more potent than isopentenyl diphosphate (IPP) from the vertebrate pathway (Amslinger et al., 2007; Eberl et al., 2003). Despite this difference in sensitivity, Vγ9Vδ2 T cells activate in response to IPP accumulated in certain primary cancers and cancer cell lines, such as human B cell lymphoma Daudi cells (Gober et al., 2003; Vantourout et al., 2009). This innate pAg-dependent anti-cancer activity can be exploited and amplified by a variety of methods. Amino-bisphosphonates (ABPs), such as zoledronate, and alkylamines specifically activate Vγ9Vδ2 T cells by inhibition of the IPP metabolizing enzyme, farnesyl diphosphate synthase (FDPS), thus increasing intracellular IPP levels (Gober et al., 2003; Li et al., 2009; Thompson et al., 2006). Alternative methods are based on previous discovery that butyrophilin 3A1 (BTN3A1) is mandatory for pAgs Vγ9Vδ2 T cell activation (Harly et al., 2012). Butyrophilins are a family of transmembrane (TM) proteins of which 8 (BTN1A1, BTN2A1/2A2, BTN3A1/3A2/3A3, MOG, and BTNL2) are located in the major histocompatibility complex (MHC) class I region of human chromosome 6. They are structurally similar to the B7 family, possessing immunoglobulin (Ig)C-IgV extracellular domains, a single-pass TM domain, a juxtamembrane (JTM) domain, and, in most members, an intracellular B30.2 domain (Blazquez et al., 2018; Rhodes et al., 2001).

Of note, no orthologs of BTN2A1 and the BTN3A isoforms exist in rodents, consistent with the absence of pAg signaling in murine cell lines (Harly et al., 2012). The noncompeting anti-BTN3A monoclonal antibodies 103.2 and 20.1 bind to the highly conserved IgV domains of all three BTN3A isoforms (Palakodeti et al., 2012), causing either a decrease or increase of Vγ9Vδ2 T cell activation, respectively (Harly et al., 2012; Starick et al., 2017). These monoclonal antibodies (mAbs) have been instrumental in Vγ9Vδ2 T cell-based therapies (Benyamine et al., 2016) and mechanistic research into BTN3A and Vγ9Vδ2 T cell activation (Blazquez et al., 2018; Gu et al., 2017, 2018; Harly et al., 2012; Palakodeti et al., 2012; Starick et al., 2017; Wang et al., 2019; Yang et al., 2019). Among the BTN3A isoforms, BTN3A1 is unique in that its intracellular B30.2 domain binds pAgs (Compte et al., 2004; Sandstrom et al., 2014), while its intracellular JTM domain performs a critical function in BTN3A homodimerization and heterodimerization via predicted coiled-coil structures that also act as rods for correct B30.2 domain spacing (Peigné et al., 2017; Wang et al., 2019). Conformational changes in the JTM domain, induced by pAgs binding at the B30.2 domain, are involved in T cell activation (Yang et al., 2019).

Further information on the mechanism of pAg activation of Vγ9Vδ2 T cells was obtained from studies using transgenic human and mouse reporter cells expressing a Vγ9Vδ2 TCR. Studies from such murine reporter cells have shown that pAg activation is critically dependent on BTN3A1 expression in APCs (tumor or infected cells) and not in effector cells (Harly et al., 2012). In addition, studies from human cells showed that both cell-to-cell contact and the Vγ9Vδ2 TCR are required for Vγ9Vδ2 T cell activation (Morita et al., 1995; Wang et al., 2010). However, scarce evidence exists to suggest that BTN3A1 directly interacts with the Vγ9Vδ2 TCR (Harly et al., 2012; Sandstrom et al., 2014). Indeed, previous studies have shown that BTN3A1 transfection alone failed to enable pAg reactivity, unless cells also contained human chromosome 6 (Riaño et al., 2014). Recently, BTN2A has emerged as the factor previously located on Chr6 and was reported to bind the Vγ9Vδ2 TCR (Karunakaran et al., 2020; Rigau et al., 2020). Two BTN2A genes exist, *BTN2A1* and *BTN2A2*, both located within a cluster that encompasses the *BTN3A* locus, and both encoding proteins containing a B30.2 domain (Rhodes et al., 2001). BTN2A1 directly binds the Vγ9 chain, and mutagenesis and structure modeling approaches mapped this interaction to the germline-encoded region between CDR2 and CDR3 of the Vγ9 chain (Karunakaran et al., 2020; Rigau et al., 2020). However, the B30.2 domain of BTN2A1 was not found to bind IPP (Rigau et al., 2020).·

In this study, we showed that BTN2A1 is a limiting factor for both pAg-driven γδ T cell cytotoxicity against cancer cells and BTN3A1 export to the plasma membrane. Using fluorescence resonance energy transfer (FRET) and proximity ligation assay (PLA) approaches, we demonstrated that BTN3A1/BTN2A1 interaction is enhanced by pAgs, emphasizing that crosstalk between BTN3A1 and BTN2A1 is essential for pAg-induced Vγ9Vδ2 T cell cytotoxicity against tumor cells. Interestingly, BTN2A2 was found insufficient for enabling Vγ9Vδ2 T cell functions. Additionally, we developed anti-BTN2A1 mAbs and elaborated a proof-of-concept of their ability to modulate Vγ9Vδ2 T cell degranulation and cancer cell killing. Finally, we established a correlation between BTN2A1 expression in cancer cells and the bisphosphonate-induced Vγ9Vδ2 T cell response.

RESULTS

BTN2A expression at the plasma membrane of target cells is required to trigger Vγ9Vδ2 T cell cytotoxicity

To assess whether BTN2A expression at the plasma membrane was required to trigger Vγ9Vδ2 T cell cytotoxicity against cancer cells, CRISPR-Cas9-mediated inactivation of BTN2A1/2A2 isoforms was performed in Daudi (B lymphoblast) and K562 (chronic myelogenous leukemia) cell lines to generate BTN2A knockout (BTN2AKO) cells. The absence of both BTN2A isoforms in Daudi and K562 BTN2AKO cells was confirmed by flow cytometry (Figure 1A). As expected, endogenous BTN3A expression was detected in BTN2AKO and control cells transduced with an irrelevant CRISPR (Irr-CRISPR). BTN2AKO cells were co-cultured with Vγ9Vδ2 T cells expanded from healthy donor peripheral blood mononuclear cells (PBMCs), with or without bacterial or synthetic pAgs (HMBPP and bromohydrin pyrophosphate [BrHPP], respectively), zoledronate, or BTN3A agonist mAb 20.1, then Vγ9Vδ2 T cell degranulation (extracellular CD107 expression) and intracellular tumor necrosis factor (TNF)-α and interferon (IFN)γ were assessed. As expected, co-culture of Vγ9Vδ2 T cells with control cells (Irr-CRISP) expressing BTN2A led to Vγ9Vδ2 T cell degranulation as well as IFNγ and TNF-α production in all conditions (Figures 1B–1D). In contrast, both Vγ9Vδ2 T cell effector functions were totally impaired in co-cultures with BTN2AKO cells, whatever the stimuli (Figures 1B–1D). Basal Vγ9Vδ2 T cell degranulation and cytokine production were also impaired in co-cultures with BTN2AKO cells (Figures 1B–1D). Consistently, in co-cultures with Vγ9Vδ2 T cells, apoptosis of BTN2AKO cells was significantly lower as compared to their wild-type counterpart (Figure S1). These results show that BTN2A expression in target cancer cells is required to trigger Vγ9Vδ2 T cell cytotoxicity.

BTN3A1 requires BTN2A1, but not BTN2A2, expression in target cells to trigger human Vγ9Vδ2 T cell cytotoxicity

Two different BTN2A isoforms exist in humans (2A1/2A2). In order to determine the involvement of these isoforms in triggering Vγ9Vδ2 T cell cytotoxicity, each isoform was reconstituted in HEK293T cells devoid of both BTN2A isoforms (BTN2AKO) using lentiviral transduction (Figures 2A, 2B, and S2). After restoring BTN2A isoforms in BTN2AKO cells (BTN2AKO+2A1, BTN2AKO+2A2, and BTN2AKO+2A1+2A2), Vγ9Vδ2 T cell degranulation was assessed with or without zoledronate. As shown in Figure 2C, restoration of BTN2A1 expression in BTN2KO target cells was sufficient to trigger Vγ9Vδ2 T cell degranulation. No such effect was observed when BTN2A2 alone was restored in BTN2AKO target cells. Although BTN2A2 expression at the plasma membrane was lower compared to BTN2A1 (Figure S2B), both BTN2A isoforms were readily detectable at higher levels than wild-type HEK293T cells, which precludes that lower BTN2A2 expression could explain its inability to trigger Vγ9Vδ2 T cell degranulation. When compared to BTN2A1 alone, no additional/synergistic effect on Vγ9Vδ2 T cell degranulation was

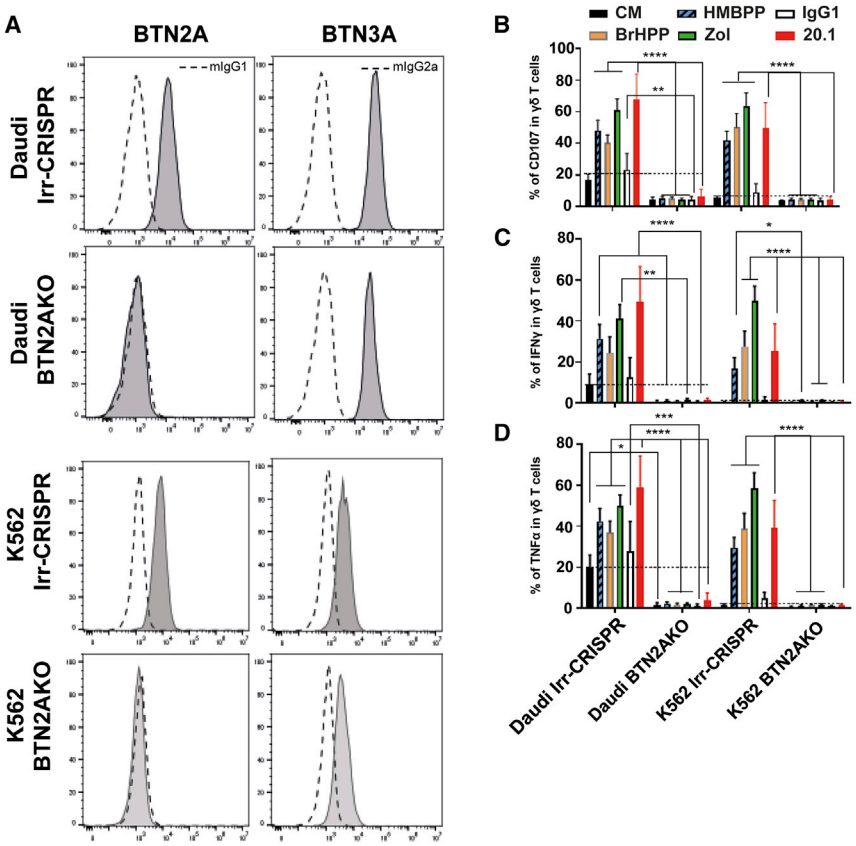

Figure 1. Plasma membrane expression of BTN2A in target cancer cell lines is required to trigger the cytotoxic response of Vγ9Vδ2 T cells

(A) CRISPR-Cas9-mediated inactivation of BTN2A1/2A2 isoforms was performed in Daudi (Burkitt lymphoma) and K562 (chronic myelogenous leukemia) cell lines, and BTN2A and BTN3A expression levels were assessed by flow cytometry, as indicated.

(B–D) Vγ9Vδ2 T cells expanded from healthy donor PBMCs (n = 6) were co-cultured with Daudi cells (effector-to-target cell [E:T] ratio of 1:1) with or without addition of BrHPP (1 μM), HMBPP (0.1 μM), zoledronate (45 μM), anti-BTN3A 20.1, or mIgG1 (10 μg/mL), as indicated.

Vγ9Vδ2 T cell degranulation (%CD107ab$^+$ cells) and intracellular TNF-α and IFNγ, respectively, were assessed after 4 h incubation in the presence of GolgiStop and analyzed by flow cytometry. CM, culture medium. *p < 0.05, **p < 0.01, ***p < 0.001, ****p < 0.0001, by two-way ANOVA with Sidak's multiple comparison test. See also Figure S1.

observed when both isoforms were re-introduced in target BTN2KO cells (Figure 2C). Results show that only BTN2A1 expression in target cells is required for Vγ9Vδ2 T cell cytotoxicity.

BTN2A1 and BTN3A1 collaborate for plasma membrane export and Vγ9Vδ2 T cell cytotoxicity

It was previously shown that BTN3A1 export to the plasma membrane is tightly regulated and enhanced by BTN3A2 expression (Vantourout et al., 2018). We sought to determine whether BTN2A1 action on Vγ9Vδ2 T cell cytotoxicity was dependent on plasma membrane exposure. Hence, we quantified the number of BTN2A1 and BTN3A molecules exposed at the plasma membrane and after membrane permeabilization (intracellular staining) in BTN2AKO/BTN3AKO cells in which BTN2A1 and all BTN3A isoforms were expressed alone or in combination. As shown in Figure 2D, reconstitution of BTN2A1 or either BTN3A isoform alone led to a heterogeneous expression pattern at the plasma membrane that contrasted to reconstitution of BTN2A1 along with either BTN3A isoform that led to more homogeneous staining profiles and higher mean fluorescence intensities (MFIs) for both proteins. Plasma membrane exposure, as depicted by the ratio between extracellular and intracellular relative number of BTN molecules per cell, showed that a lower BTN2A1 extracellular/intracellular ratio was strongly enhanced by BTN3A1 co-expression, and to a lesser extent by BTN3A2 and BTN3A3 (Figures 2E and S2C). Conversely, BTN2A1 co-expression led to enhanced plasma membrane expression of BTN3A2 and BTN3A3 (Figure 2F). Consistent with this observation, BTN2AKO Daudi cells displayed fewer BTN3A molecules compared to their Irr-CRISPR counterpart (Figure S2E). We then assessed the ability of each BTN2A1/BTN3A combination to trigger Vγ9Vδ2 T cell degranulation (Figures 2G and S2D) and found that only the BTN2A1/BTN3A1 combination allowed responsiveness to zoledronate. These results indicate that BTN2A1 and BTN3A1 trafficking to the plasma membrane are linked, and that BTN2A1 is mandatory for BTN3A1-mediated pAg sensing by Vγ9Vδ2 T cells.

BTN2A1 and BTN3A1 interaction is enhanced by pAgs

To determine whether BTN2A1 and BTN3A1 form protein complexes, we performed co-immunoprecipitation (co-IP) experiments after BTN2AKO/3AKO HEK293T cell transfection with Myc-tagged BTN2A1, GFP-tagged BTN3A1, or both. As shown in Figure 3A (and Figure S3A), Myc-BTN2A1 was detected after GFP-BTN3A1 immunoprecipitation in cells expressing both tagged proteins, but not in their mock controls. Flow cytometry assessment of the FRET signal was used to assess homomeric and heteromeric interactions between different BTN2A and BTN3A isoforms in live cells (Figures 3B and S3B). A positive FRET signal indicated that BTN2A1 and BTN2A2 were able to form homodimers, as well as all BTN3A isoforms. However, only BTN2A1 was found to interact with all BTN3A isoforms. In contrast, BTN2A2 interacted with BTN3A1 only. No interaction between BTN2A1 and BTN2A2 was observed. To identify BTN2A1/2A2 protein domains involved in interactions with BTN3A1, FRET experiments using wild-type BTN3A1 and different BTN2A1 or BTN2A2 mutated domains (ectodomain [EC], B30.2, JTM, TM) were tested. As observed in Figures 3C

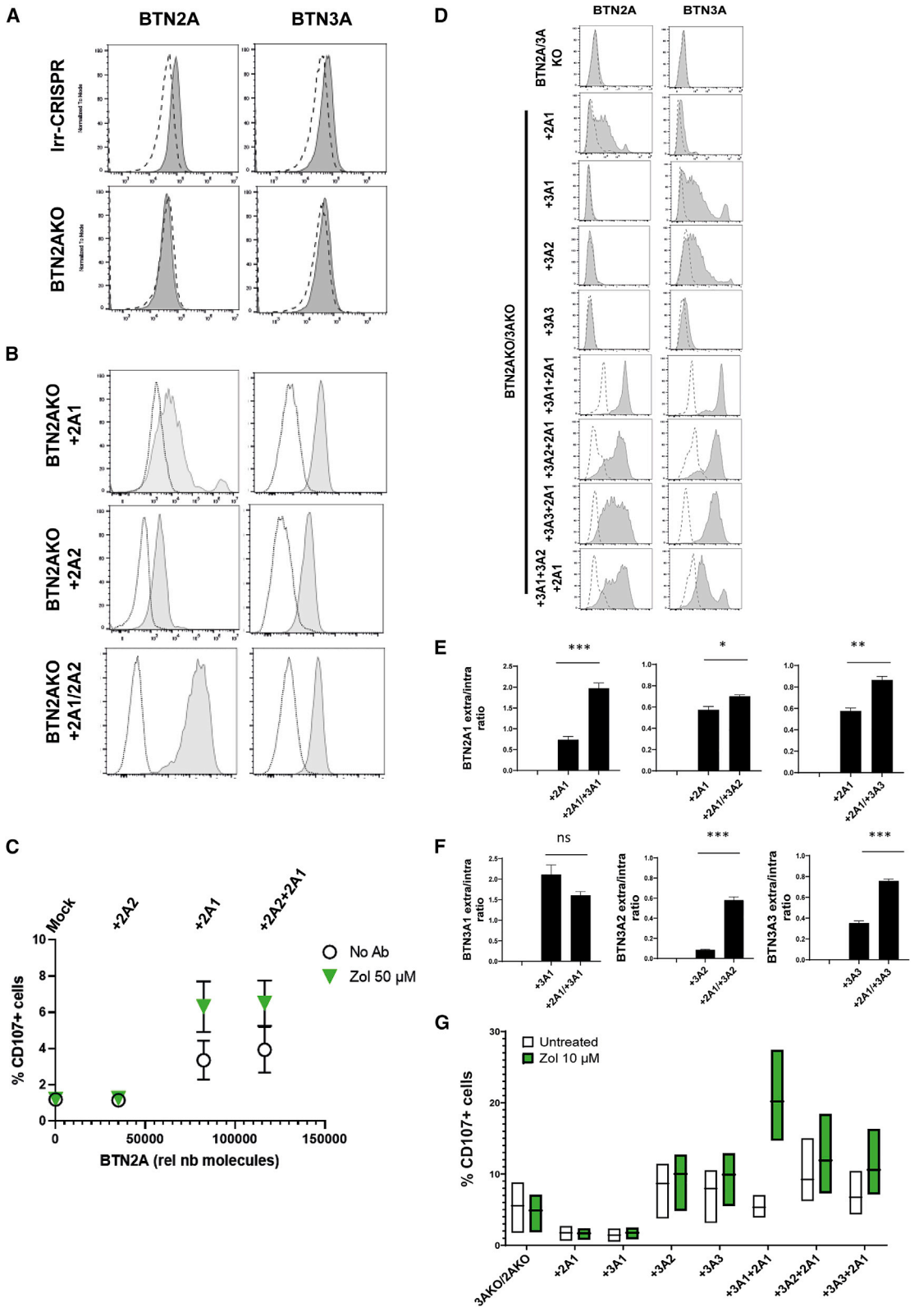

(legend on next page)

and S3C, regarding the BTN2A1/BTN3A1 complex (black bars), replacement of the BTN2A1 EC (2A1-mEC) disrupted interaction with BTN3A1, whereas for BTN2A2 (yellow bars), deletion of the BTN2A2 B30.2 domain prevented interaction with BTN3A1.

Treatment with zoledronate enhances BTN2A1/BTN3A1 interaction observed by FRET (Figure 3D). Zoledronate-dependent enhancement relies on the BTN3A1 B30.2 domain. In line with data shown in Figures 3C and S3D, deletion of the B30.2 domains of BTN3A1 did not prevent the interaction with BTN2A1. However, and more surprisingly, deletion of the B30.2 domain of BTN2A1 abolished zoledronate-induced degranulation of Vγ9Vδ2 T cells to the same extent as did deletion of the BTN3A1 B30.2 domain (Figures 3E and S3E).

Because co-IP and FRET do not allow to restrict the analysis of interactions to the plasma membrane, we used microscopy-based PLA to interrogate BTN2A1/BTN3A1 interaction at the plasma membrane. Quantification of molecules proximity was performed at steady state or after treatment with zoledronate. As shown in Figures 3F, S3F, and S3G, the PLA approach confirmed BTN2A1/BTN3A1 interaction and its enhancement by zoledronate at the plasma membrane. Altogether, these data show that BTN2A1 and BTN3A1 interact through their ECs. Moreover, BTN2A1/BTN3A1 interaction appeared to be enhanced by zoledronate treatment.

Ectopic expression of BTN2A1 and BTN3A1 in murine target cells empowers murine T cells with Vγ9Vδ2TCR responsiveness

It was previously shown that BTN3A1 alone was insufficient to restore pAg-mediated activation through the human Vγ9Vδ2 MOP TCR expressed in a murine T cell hybridoma (Riaño et al., 2014; Starick et al., 2017). To test whether ectopic expression of human BTN2A1 in murine fibroblasts was able to drive Vγ9Vδ2TCR responsiveness, the murine Vγ9Vδ2 MOP TCR reporter T cell hybridoma was co-cultured with mouse NIH-3T3 fibroblasts transfected with both BTN2A isoforms, alone or in combination with BTN3A isoforms with or without HMBPP treatment (Figures 4A and S4). Consistently with results obtained in the human setting, only concomitant expression of BTN2A1 and BTN3A1 allowed HMBPP responsiveness of murine Vγ9Vδ2 MOP TCR reporter cells, as assessed by mouse interleukin (mIL)-2 secretion measured by ELISA. BTN2A1/BTN3A1 expression in NIH-3T3 cells granted dose-dependent activation of murine Vγ9Vδ2 MOP TCR reporter cells by HMBPP and anti-BTN3A agonist 20.1 mAbs (Figures 4B and 4C). Moreover, increasing concentrations of an anti-BTN3A antagonist mAb (103.2) inhibit HMBPP-driven mIL-2 production (Figure 4D). As in assays with HEK cells, B30.2 domains of BTN2A1 and BTN3A1 were required for HMBPP responsiveness in the murine setting (Figures S4B–S4D). Altogether, these results show that ectopic expression of BTN2A1 and BTN3A1 in murine target cells is required and sufficient to empower murine T cells with Vγ9Vδ2 TCR responsiveness to pAgs.

Vγ9Vδ2 T cell function can be modulated using anti-BTN2A1 mAbs

Vγ9Vδ2 T cell anti-tumor activity involves degranulation and release of perforin and granzyme, as well as cytokine secretion, resulting in cancer cell killing. To determine whether BTN2A1 targeting was suitable to modulate Vγ9Vδ2 T cell anti-tumor responses, we generated seven anti-BTN2A1 mAbs. Two of these mAbs shared identical VH/VL sequences (8.15 and 8.16, data not shown). Binding of anti-BTN2A1 mAbs *in cellulo* on HEK BTN2AKO+2A1 cells and affinity as assessed by biolayer interferometry (BLI) are shown in Figures S5A and S5B. BLI-based binning assays identified three different epitope bins covered by our anti-BTN2A1 mAbs (Figure S5C). Furthermore, we tested the effect of anti-BTN2A1 mAbs on Vγ9Vδ2 T cell degranulation against Daudi cells with or without zoledronate or anti-BTN3A agonist mAb 20.1 (Figure 5A). As expected, in co-cultures with Daudi cells alone, the mean (±SEM) of basal Vγ9Vδ2 T cell degranulation was 23.1% ± 5.84% $CD107^+$ cells. These results remained unchanged in the presence of isotype controls (23.1% ± 5.42% and 24.9% ± 5.6% for IgG1 and IgG2a, respectively), and they were enhanced by the addition of mAb 20.1 (71.8% ± 4.7%). Zoledronate led to up to a 3-fold increase of Vγ9Vδ2 T cell degranulation against Daudi cells in all control conditions ($p \leq 0.05$) but did not add to mAb 20.1 stimulation. Strikingly, six out of seven anti-BTN2A1 mAbs, namely clones 4.15, 8.15, 8.16, 7.28, 7.48, and 5.28, significantly inhibited basal Vγ9Vδ2 T cell degranulation against Daudi cells up to 17-fold, and all of these clones but the 7.28 were able to inhibit Vγ9Vδ2 T cell degranulation against Daudi cells in the presence of zoledronate or mAb 20.1 (Figure 5A). To determine whether anti-BTN2A1 mAbs modulated cancer cell killing induced by zoledronate and anti-BTN3A agonist 20.1, Vγ9Vδ2 T cells were co-cultured with HL-60 cells in the presence of zoledronate or 20.1 mAb with or without anti-BTN2A1 mAbs. Apoptosis inhibition was estimated by flow cytometry analysis of caspase-3/7 cleavage in HL-60 cells. Consistent with Vγ9Vδ2 T cell degranulation,

Figure 2. BTN2A1 and BTN3A1 expression in target cells allows triggering of human Vγ9Vδ2 T cell cytotoxicity

HEK293T cells transduced with an irrelevant CRISPR (Irr-CRISPR) guide or a guide targeting both BTN2A isoforms (BTN2AKO) (A and B) or guides targeting all BTN2A and BTN3A isoforms (BTN2AKO/3AKO) (D–F); BTN2AKO cells were transduced with lentiviruses encoding BTN2A1 (+2A1), BTN2A2 (+2A2), or both (+2A1/2A2, A, B, and C), and BTN2AKO/3AKO cells were transduced with lentiviruses encoding BTN2A1 (+2A1) or each BTN3A isoform alone or (D and F) in combination with BTN2A1, or with an empty lentiviral vector (mock), as indicated. (A and D) BTN2A1 and BTN3A expression were assessed by flow cytometry (D) and the ratio of extracellular/intracellular BTN2A1 or BTN3A molecule numbers was calculated after quantification using a CellQuant assay (E and F, respectively) using 7.48 (an anti-BTN2A antibody generated in this study, the properties of which are described elsewhere in this manuscript) and 103.2 mAbs, respectively. *$p < 0.05$, **$p < 0.01$, ***$p < 0.001$, ****$p < 0.000$, by two-tailed unpaired t test. (C and G) Vγ9Vδ2 T cells expanded from healthy donor PBMCs (n = 2) were co-cultured with BTN2AKO cells (E:T ratio of 1:1) transduced with an empty pLV vector (mock), or the indicated BTN2A or 3A isoform combinations with or without addition of zoledronate (50 μM), as indicated, and Vγ9Vδ2 T cell degranulation (%$CD107^+$ cells) was assessed after 4 h by flow cytometry. (C) Chart illustrates correlation between Vγ9Vδ2 T cell degranulation (%$CD107ab^+$ cells, y axis) and the number of BTN2A molecules (as assessed with 7.48; x axis). Linear regression was used to calculate the correlation between %$CD107^+$ cells and the number of BTN2A molecules. *$p < 0.05$, **$p < 0.01$, ***$p < 0.001$, ****$p < 0.0001$. Statistics in (E) are compared to +2A1 cells. See also Figure S2.

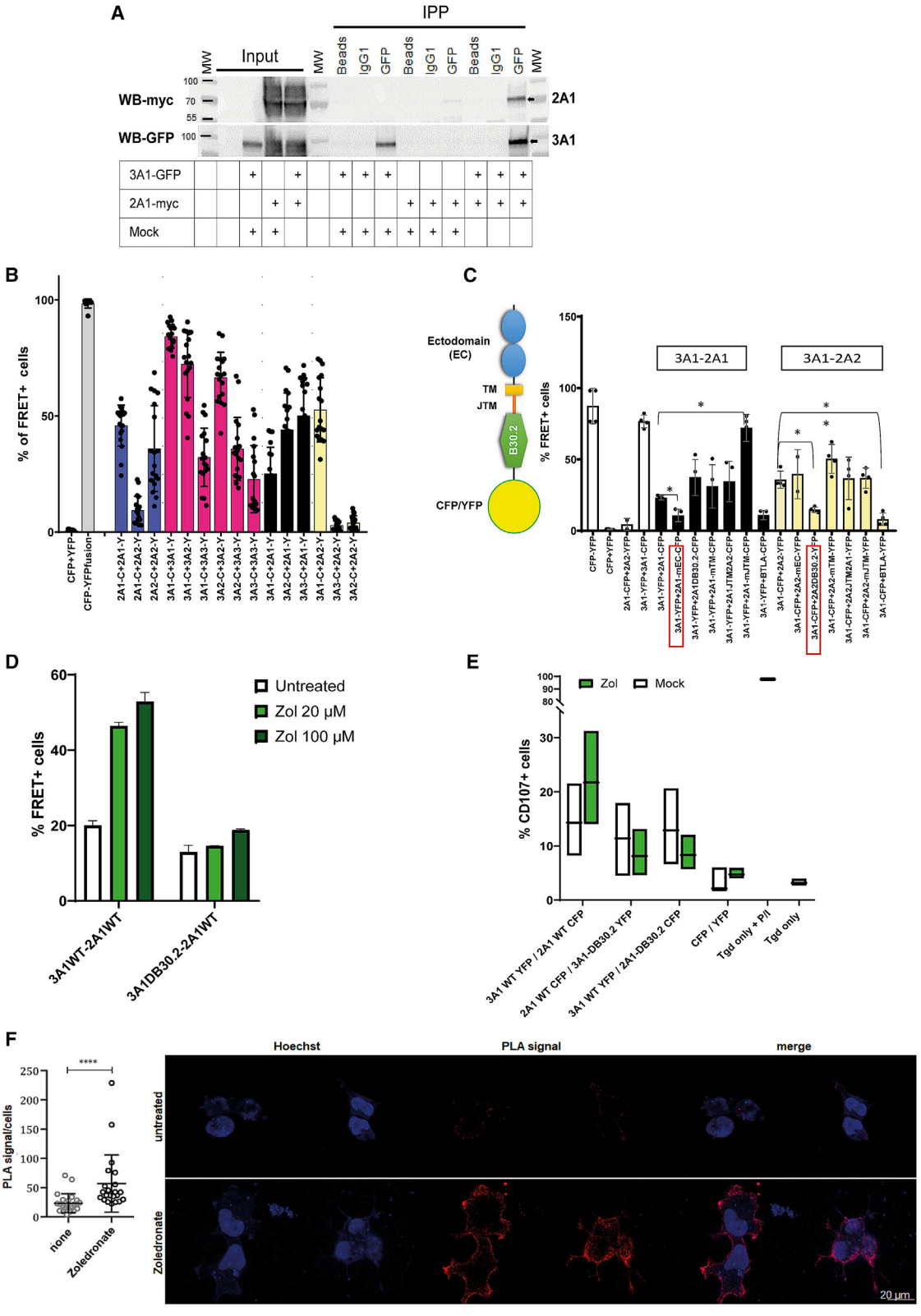

(legend on next page)

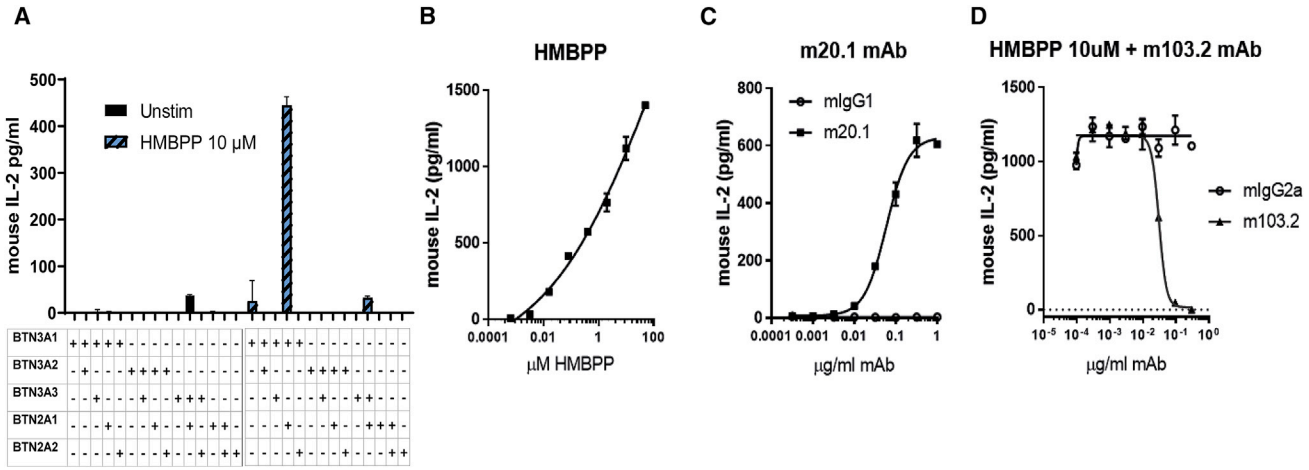

Figure 4. BTN2A1 and BTN3A1 expression in cognate cells is necessary and sufficient to empower murine T cells with Vγ9Vδ2TCR responsiveness to phosphoantigens

(A) 53/4 mouse T cell hybridoma expressing TCRVγ9Vδ2 MOP was co-cultured overnight (ratio 1:1) with NIH-3T3 murine fibroblasts transfected with the indicated BTN3A- or BTN2A-encoding plasmids, with or without HMBPP (10 μM); (B and C) or with plasmids encoding BTN2A1 and BTN3A1, with increasing doses of HMBPP or anti-BTN3 agonist 20.1 mAb, respectively; and (D) or in the presence of HMBPP and increasing doses of anti-BTN3A antagonist 103.2 mAb. Secreted mIL-2 was measured by ELISA and used as a readout in all panels. See also Figure S4.

anti-BTN2A1 mAbs abrogated zoledronate and anti-BTN3A 20.1-induced apoptosis with different efficiencies (Figure 5B). For each anti-BTN2A1 clone, the level of apoptosis inhibition after zoledronate and 20.1 treatment were correlated (Figure 5C). Anti-BTN2A1 mAbs inhibited perforin and granzyme B release in the same settings (Figure S5D). The anti-BTN2A1 7.48 mAb was the clone with the strongest inhibitory potential. Increasing concentrations of anti-BTN2A1 7.48 abrogated Vγ9Vδ2 T cell responses against Daudi cells in the presence of HMBPP or 20.1 in terms of degranulation (Figure 5D; half-maximal inhibitory concentration [IC_{50}] = 0.067 and 0.056 μg/mL, respectively), TNF-α (Figure 5E, IC_{50} = 0.094 and 0.082 μg/mL), and IFNγ (Figure 5F, IC_{50} = 0.114 and 0.13 μg/mL) secretion.

Anti-BTN2A1 7.48 was able to inhibit HMBPP-induced mIL-2 secretion in mouse Vγ9Vδ2 MOP TCR reporter cells co-cultured with BTN2A1/BTN3A1-expressing NIH 3T3 cells (Figures S5E and S5F). A concentration of 10 μg/mL anti-BTN2A1 7.48 mAb led to a strong inhibition of mIL-2 production. Although high concentrations of HMBPP were used to trigger activation, mIL-2 production remained very low in the presence of 7.48 mAb (Figure S5E). Reciprocally, in this setting anti-BTN2A1 7.48 inhibited mIL-2 production in a dose-dependent manner (Figure S5F).

Anti-BTN2A1 antagonist mAb inhibits cytotoxic function of activated Vγ9Vδ2 T cells

3D spheroids were used to assess the ability of the anti-BTN2A1 7.48 antagonistic mAb to inhibit Vγ9Vδ2 T cell killing of cancers cells. Spheroids derived from the endometrial cancer cell line Ishikawa were cultured with Vγ9Vδ2 T cells from different healthy donors and treated with anti-BTN3A alone (20.1) or in combination with the anti-BTN2A1 7.48 antagonistic mAb. Apoptosis of Ishikawa cells within spheroids was evaluated by caspase-3/7 flow cytometry. Ishikawa cell spheroid apoptosis and release of perforin and granzyme B were observed in the presence of anti-BTN3A (20.1) and γδT cells (Figures 6A, 6B, and S6A–S6C). However, apoptosis and perforin/granzyme B release were inhibited when spheroid co-cultures were treated concomitantly with mAb 7.48. These results show that anti-BTN2A1 antagonist mAb 7.48 inhibits cytotoxic function of activated γδT cells in conditions closer to the tumor setting.

To determine whether BTN2A1 targeting by a mAb allowed modulation of Vγ9Vδ2 T cell cytotoxicity against primary cancer cells, we assessed the ability of anti-BTN2A1 7.48 mAb to modulate a Vγ9Vδ2 T cell cytotoxic response against primary acute myelocytic leukemia (AML) blasts in terms of degranulation,

Figure 3. BTN2A1 and BTN3A1 protein interactions

(A) BTN2AKO/BTN3AKO HEK293T cells were transfected with the indicated plasmids (bottom table), before cell lysis and immunoprecipitation (IPP) with anti-GFP (targeting 3A1-GFP fusion) antibody and western blotting with anti-myc (for 2A1-myc fusion, top image) or anti-GFP (bottom image).

(B–D) Fluorescence resonance energy transfer (FRET) assays assessing homodimeric and heterodimeric interactions between different BTN2A and BTN3A isoforms (B), wild-type BTN3A1 with different BTN2A1 or BTN2A2 domain shuffled constructs (C, and see Figure S1B), and impact of zoledronate treatment (20 or 100 μM, overnight [O/N]) and of B30.2 domain shuffling on BTN2A1/BTN3A1 dimer formation (D).

(E) Expanded Vγ9Vδ2 T cells (n = 3) were co-cultured, in the presence or absence of zoledronate (50 μm), with BTN2AKO/3AKO cells (1:1) transfected with: (i) wild-type BTN3A1-YFP/wild-type BTN2A1-CFP, or (ii) wild-type BTN2A1-CFP/B30.2-deleted (DB30.2) BTN3A1-YFP, or (iii) wild-type BTN3A1-YFP/BTN2A1-B30.2 deleted (DB30.2)-CFP fusion constructs. Percentages of $CD107^+$ Vγ9Vδ2 T cells were assessed after 4h of co-cultures. A one-way ANOVA test was used for comparison. *p < 0.05; **p < 0.01, ****p < 0.0001.

(F) (left) Number of PLA signal per cell on WT HEK-293T transiently transfected with tagged BTN3A1 and BTN2A1 plasmids. Mann-Whitney: ****p < 0.001. (right).Representative images on untreated cells (top) or cells treated with zoledronate (bottom) for 4 h. Scale bar: 20 μm.

See also Figures S3 and S4.

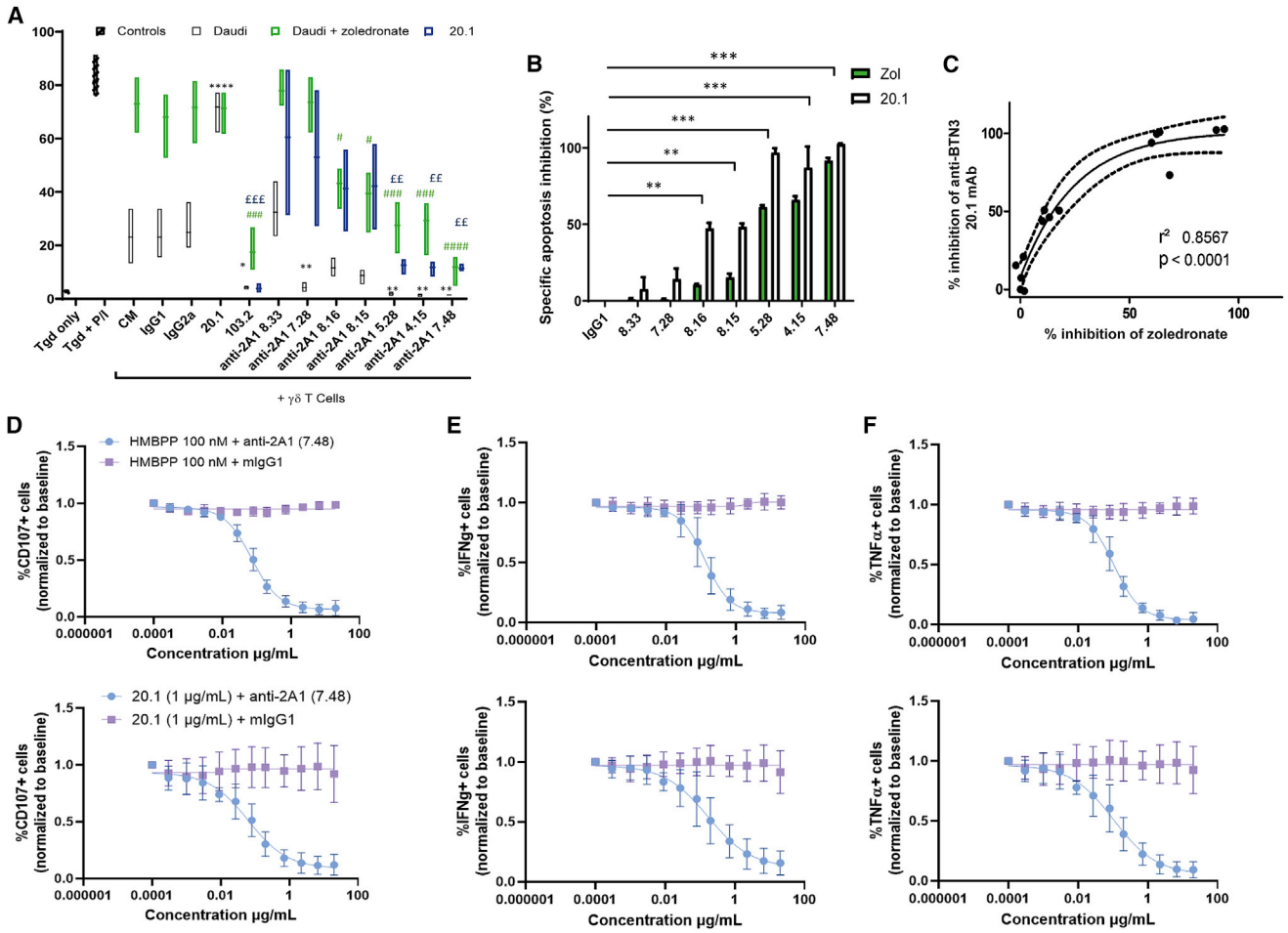

Figure 5. Vγ9Vδ2 T cell function can be modulated using an anti-BTN2A1 mAb

(A) Vγ9Vδ2 T cell degranulation against Daudi cells with or without zoledronate, and with or without the indicated anti-BTN3A (20.1 and 103.2) and anti-BTN2A1 mAbs. $^{*,\#,£}p < 0.05$, $^{**,\#\#,££}p < 0.01$, $^{***,\#\#\#,£££}p < 0.005$, $^{****,\#\#\#\#}p < 0.0001$ compared to control IgG against Daudi alone, + zoledronate, or +20.1, respectively, using one way-ANOVA with a Holm-Sidak comparison test.

(B) Vγ9Vδ2 T cells were co-cultured with HL-60 cells (the E:T ratio is 5:1) in the presence of zoledronate (50 µM) or 20.1 mAb (10 µg/mL) with or without anti-BTN2A mAbs or control IgG1 (10 µg/mL). Apoptosis inhibition was estimated by flow cytometry analysis of caspase-3/7 cleavage in HL-60 cells. $^{*}p < 0.05$, $^{**}p < 0.01$, $^{***}p < 0.001$, $^{****}p < 0.0001$, by one-way ANOVA test.

(C) Correlation between HL-60 apoptosis inhibition by anti-BTN2A 7.48 mAb upon zoledronate (x axis) and 20.1 mAb (y axis) treatment. 95% confidence interval of the best-fit nonlinear exponential regression is depicted by the dotted line.

(D–F) Vγ9Vδ2 T cell degranulation (D) and TNF-α (E) and IFNγ (F) secretion against Daudi cells in the presence of HMBPP (top) or anti-BTN3A agonist 20.1 (bottom) without anti-BTN2A 7.48 (10 µg/mL); data were normalized to baseline (HMBPP or 20.1 without antibody).

See also Figure S5.

cytokine production, perforin/granzyme B release, and cell killing. As shown in Figures 6C, 6D, and S6D–S6I, anti-BTN2A1 7.48 mAb was able to efficiently inhibit Vγ9Vδ2 T cell degranulation, TNF-α/IFNγ production, perforin/granzyme B release, as well as killing of primary AML blasts, even after 20.1 and zoledronate activation.

BTN2A1 expression at the plasma membrane correlates with Vγ9Vδ2 T cell responsiveness to pAgs

To determine whether Vγ9Vδ2 T cell cytotoxicity was dependent on the number of BTN2A1 molecules available at the plasma membrane of target cells, Vγ9Vδ2 T cell degranulation against eight different cancer cell lines (HL-60, Daudi, A549, PC3, HCT116, MDA-MB-231, K562, and Panc-1) was assessed with or without zoledronate using flow cytometry (Figures 6E and 6F). Linear regression was used to determine the correlation between the number of BTN2A1 molecules in target cells and the percentage of $CD107^{+}$ Vγ9Vδ2 T cells. No significant correlation was observed when looking at basal degranulation against the indicated cancer cell lines (Figure 6E). In contrast, zoledronate-induced Vγ9Vδ2 T cell degranulation was significantly correlated with the number of BTN2A1 molecules in target cells (Figure 6F). Moreover, BTN2A1 expression and caspase-3/7 cleavage after co-culture with Vγ9Vδ2 T cells in presence of zoledronate and 20.1 mAb were assessed on 10 primary AML blast samples using flow cytometry (Figures 6G and 6H). AML blasts presenting the

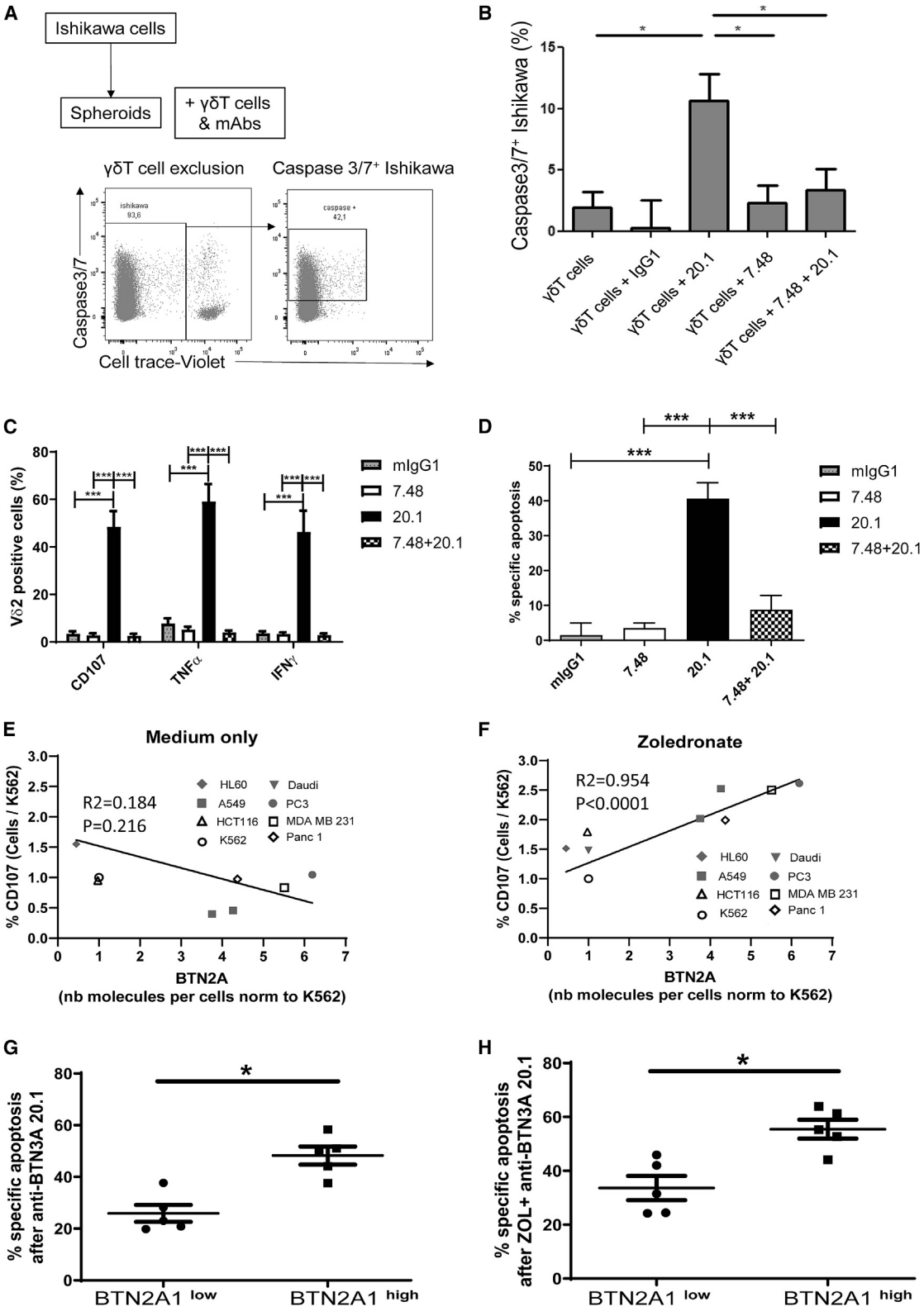

(legend on next page)

higher plasma membrane expression of BTN2A1 underwent significantly more Vγ9Vδ2 T cell-induced apoptosis than did those expressing low levels of BTN2A1. Hence, BTN2A1 expression is associated with Vγ9Vδ2 T cell cytotoxicity against both cancer cell lines and primary AML.

Anti-BTN2A1 antagonist mAbs inhibit BTN2A1/Vγ9Vδ2 TCR interaction

We sought to determine the effect of the different anti-BTN2A1 mAbs on BTN2A1/BTN3A1 interaction by using FRET. To this end, BTN2AKO/BTN3AKO HEK293T cells were transfected to express CFP/YFP-fusion BTN2A1 and BTN3A1 proteins and incubated with growing concentrations of different anti-BTN2A1 mAbs. Figure 7A shows that different anti-BTN2A1 clones had different impacts on BTN3A1/2A1 interaction. Strikingly, some Vγ9Vδ2 T cell antagonists were found to increase BTN2A1/BTN3A1 FRET signal (8.15 and 7.28), whereas others (4.15, 7.48, and 5.28) decreased it. Interestingly, the anti-BTN3A antagonist 103.2 also mildly increased the BTN2A1/BTN3A1 dimer formation, whereas the 20.1 clone showed no effect.

Finally, we investigated whether the activity of our Vγ9Vδ2 T cell antagonist anti-BTN2A1 mAbs was due to an inhibitory effect on the interaction between BTN2A1 and Vγ9Vδ2 TCR. We assessed the specific binding of Vγ9Vδ2 TCR G115 to HEK-BTN2AKO+2A1 cells and not to HEK-BTN2AKO cells (Figure 7B). Then, we determined whether anti-BTN2A1 mAbs impaired Vγ9Vδ2 TCR G115 binding to the plasma membrane of HEK-BTN2AKO+2A1 cells. To this end, HEK-BTN2AKO+2A1 cells were pre-incubated with a saturating concentration of our antagonist anti-BTN2A1 antibodies (7.48, 7.28, 4.15, 5.28, 8.15) and the neutral clone (8.33) prior to incubation with Alexa Fluor 647 (AF647)-conjugated recombinant Vγ9Vδ2 TCR G115, and Vγ9Vδ2 TCR binding was assessed by flow cytometry. As shown in Figure 7C, while the neutral (8.33) and weak inhibitor (7.28) did not affect Vγ9Vδ2 TCR binding to BTN2A1, our stronger inhibitors, namely, 7.48, 4.15, 5.28, and 8.15, completely abolished BTN2A1/Vγ9Vδ2 TCR interaction. Similar results were obtained when looking at the binding of Vγ9Vδ2 TCR G115 tetramers to Daudi cells in the presence of our anti-BTN2A1 mAbs (Figures S7A and S7B), and when using ELISA to assess Vγ9Vδ2 TCR-Fc binding to BTN2A1-His, and the competition of anti-BTN2A mAbs for this binding (Figures S7C and S7D).

Hence, these data show that blocking Vγ9Vδ2 TCR binding is associated with the antagonist effect of our anti-BTN2A1 mAbs, and that disruption of the BTN2A1/BTN3A1 dimer is not the only possible way to modulate Vγ9Vδ2 T cell function.

DISCUSSION

In this study, we demonstrate that the interaction between BTN3A1 and BTN2A1, but not BTN2A2, is essential for the cytotoxic response of primary Vγ9Vδ2 T cells against cancer cells. These properties were identified not only in transfected models but also in primary human tumors. A link between BTN2A1 expression and pAgs triggering of Vγ9Vδ2 T cells was also demonstrated. At the molecular level, BTN3A1 and BTN2A1 form complexes at the plasma membrane. Their co-expression is critical for BTN2A1 export to the plasma membrane, and BTN2A1 can also interact and enhance plasma membrane exposure of BTN3A2 and BTN3A3 to a lesser extent. Interestingly, BTN2A1, but not BTN2A2, interacted with BTN3A2 and BTN3A3. The interaction between BTN3A1 and BTN2A1 involves at least two major mechanisms. First, the extracellular domains of BTN2A1 were critical to its interaction with BTN3A1, as shown in FRET experiments using domain shuffled BTN2A1 constructs. In addition, pAgs were an important factor to elicit a high level of complex formation, plasma membrane export, and function.

Despite compelling data demonstrating immunoregulatory properties of BTN2A2 in rodents (Sarter et al., 2016), we did not identify a crucial function in human Vγ9Vδ2 T cells. The generation of a panel of anti-BTN2A1 mAbs allowed us to further decipher the interactions and functions of BTN2A1 and BTN3A1, with the discovery of antagonistic mAbs that inhibit Vγ9Vδ2 T cell cytotoxicity upon treatment with zoledronate or activating anti-BTN3A mAb.

Figure 6. Anti-BTN2A1 antagonistic mAb inhibits the cytotoxic function of activated Vγ9Vδ2 T cells

(A) Ishikawa cells were cultured for 7 days to obtain spheroids. CellTrace Violet (CTV)-stained Vγ9Vδ2 T cells were then added to the spheroids under the following conditions: γδT cells alone, γδT cells + mIgG1, γδT cells + 7.48, γδT cells + 20.1, or γδT cells + 7.48 and 20.1. After overnight culture with caspase-3/7 staining, spheroids were dissociated and processed for flow cytometry following the displayed gating strategy.

(B) Bar chart represents the percentage of caspase-3/7$^+$ Ishikawa cells after culture conditions detailed in (A). *$p < 0.05$. n = 4 Vγ9Vδ2 T cells donors.

(C) Bar charts represent the fraction of CD107ab$^+$, TNF-α$^+$, and IFNγ$^+$ Vγ9Vδ2 T cells (n = 3) after a 4-h co-culture (E:T ratio of 1:1) with primary AML blasts (n = 6) either with isotype control or anti-BTN2A1 7.48 mAb and/or anti-BTN3A 20.1 (10 μg/mL).

(D) Results from three independent experiments are depicted and expressed as mean ± SEM. Caspase-3/7 expression is shown on primary AML blasts (n = 12) after coculture for 3 h 30 min with Vγ9Vδ2 T cells (n = 3) with an E:T ratio of 15:1. Cells were treated with isotype control or anti-BTN2A1 7.48 mAb and/or anti-BTN3A 20.1 (10 μg/mL).

(C and D) AML blasts were preincubated overnight in medium. Results from six independent experiments are depicted, expressed as mean ± SEM, by non-parametric paired ANOVA repeated-measures test with a Bonferonni post hoc test. ***$p < 0.001$.

(E and F) Fraction of CD107$^+$ Vγ9Vδ2 T cells triggered by the indicated cancer cell lines was assessed by flow cytometry. Graphs illustrate correlation between Vγ9Vδ2 T cell degranulation (%CD107$^+$ cells, y axis) against the indicated cancer cell lines, in the absence or presence of zoledronate (50 μM, G and H, respectively), and the number of BTN2A molecules (as assessed with 7.48; x axis). Linear regression was used to calculate the correlation between %CD107$^+$ cells and the number of BTN2A molecules. Results from two separate experiments were merged through normalization to the K562 cell line, present in both experiments.

(G and H) Caspase-3/7 expression on primary AML blasts (n = 10) after a coculture for 3 h 30 min with Vγ9Vδ2 T cells (E:T ratio of 15:1). Cells were treated with anti-BTN3A 20.1 agonist (10 μg/mL) with and without zoledronate, as indicated. The BTN2A1 expression was assessed by flow cytometry analysis and expressed as median fluorescence intensity (MFI). The statistical significance was established using the Mann-Whitney test. *$p < 0.05$.

See also Figure S6.

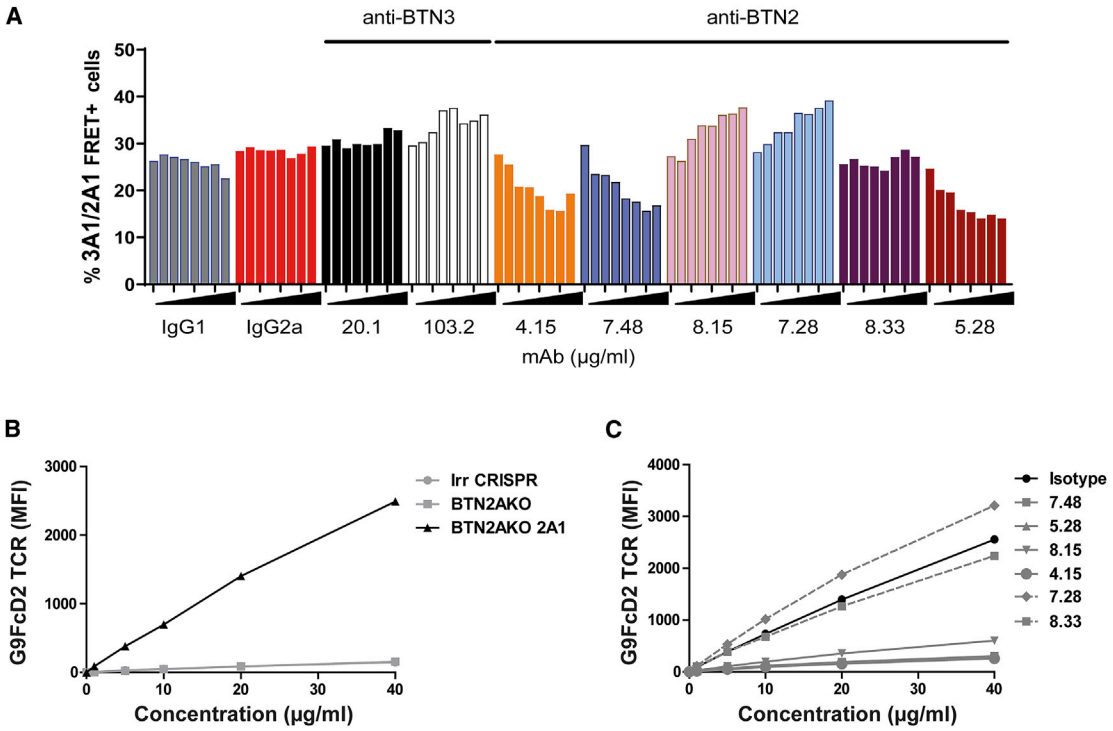

Figure 7. Anti-BTN2A1 mAbs inhibit recombinant Vγ9Vδ2 TCR binding to BTN2A1

(A) BTN2AKO/3AKO HEK293T cells were transfected with vectors encoding BTN2A1-CFP and BTN3A1-YPF, treated for 6 h with cycloheximide and bafilomycin to prevent dimer trafficking, and incubated with increasing concentrations (0–10 μg/mL) of the indicated mAbs. Graph shows the percentage of BTN2A1/BTN3A1 FRET$^+$ cells for each condition.

(B) Binding curves of recombinant Vγ9Vδ2 TCR to HEK-BTN2AKO+2A1 and HEK-BTN2AKO cells.

(C) Binding curves of recombinant Vγ9Vδ2 TCR to HEK-BTN2AKO+2A1 cells, following saturation with a panel of anti-BTN2A antibodies compared to isotype control (black).

See also Figure S7.

Using flow cytometry-based FRET experiments, we have shown that BTN2A1 was associated with BTN3A1 and to a lesser extent with BTN3A2 and BTN3A3. We have shown that interaction with BTN2A1 is the limiting factor for plasma membrane export of BTN3A2 and BTN3A3, which in turn regulate BTN3A1 trafficking (Vantourout et al., 2018), thus allowing Vγ9Vδ2 T cell activation. Consistently, the level of BTN2A1 expression at the plasma membrane in different cancer cell lines is correlated to the potency of Vγ9Vδ2 T cell degranulation against these cells (Figure 6F). In addition, primary AML blasts with high BTN2A1 expression underwent significantly more apoptosis in co-cultures with Vγ9Vδ2 T cells (Figures 6G and 6H). The initial experiments from Vantourout et al. (2018) could not address the involvement of BTN2A1 in BTN3A plasma membrane export since their BTN3AKO HEK cells expressed BTN2A1. In our experiments, not only could BTN2A1 enhance the export of all BTN3A isoforms to the plasma membrane, but also BTN3A2 and BTN3A3 isoforms reciprocally enhanced the plasma membrane exposure of BTN2A1. Reciprocally, the three BTN3A isoforms are limiting factors for BTN2A1 expression at the plasma membrane. These results suggest that changes in the expression of any of the three isoforms of BTN3A could have a consequence on BTN2A1 extracellular expression and, thus, an indirect impact on Vγ9Vδ2 T cell cytotoxicity.

Another key demonstration in this study is the impact of pAgs in BTN3A1/BTN2A1 interaction. Indeed, zoledronate treatment enhances the interaction between BTN3A1 and BTN2A1. This effect, as expected, was totally prevented by the deletion of the BTN3A1 B30.2 domain, whereas the deletion of the B30.2 domain of BTN2A1 did not (data not shown). This latter observation is in line with data from Rigau et al. (2020) showing the absence of pAgs binding to the BTN2A1 B30.2 domain. One could predict that, similar to during amino bisphosphonate treatment, an IPP intracellular increase during pathologic conditions such as malignant transformation or infection will enhance BTN3A1/BTN2A1 interaction at the plasma membrane. Whether pAg levels also increase the formation of multimers including BTN3A1, BTN2A1, and other BTN3As remains to be demonstrated (Dustin et al., 2019). Unexpectedly, deletion of the B30.2 domain of BTN2A1 was as deleterious to zoledronate-induced Vγ9Vδ2 T cell degranulation as was deletion of the BTN3A1 B30.2 domain (Figure 3E). Although the BTN2A1 B30.2 domain does directly bind to pAgs (Rigau et al., 2020), it is possible that it participates in the formation of an asymmetrical pocket along with the BTN3A1 B30.2 domain, as shown by Yang et al. (2019) for BTN3A1 homodimers.

The literature available since 2010 has shown that BTN2A2 has an immune function. First, murine BTN2A2-Fc chimeric

protein was shown to inhibit the proliferation of $CD4^+$ and $CD8^+$ T cells (Smith et al., 2010). In addition, BTN2A2-Fc on activated murine T cells was able to inhibit TCR signaling and promoted *in vitro* generation of $CD4^+CD25^+$ $Foxp3^+$ T cells (Ammann et al., 2013). Later, Sarter et al. (2016) generated Btn2a2-KO mice and showed that BTN2A2 expression, mainly on antigen-presenting cells (APCs), might negatively regulate immune functions, presumably T cell functions, which were hypothetically associated with inhibitory signals controlling T cell anti-tumor responses. Altogether, these data using different *in vitro* and *in vivo* experimental settings demonstrated the role of BTN2A2 in immunomodulation, mainly via T cell regulation in mice. Vγ9Vδ2 T cells are not present in rodents (Karunakaran et al., 2014). Data shown herein demonstrate that BTN2A2 is not required for Vγ9Vδ2 T cell function in humans (Figure 3). Whether BTN2A2 functions outside the Vγ9Vδ2 T cell compartment relying on other immune cells remains to be explored. Among the surprising observations regarding BTN2A2, we found that BTN2A2 did possess the ability to interact with BTN3A1 (Figure 6), yet it was unable to elicit Vγ9Vδ2 T cell degranulation. Whether BTN2A2 might interfere with BTN3A1/BTN2A1 interaction, compete for it, and thus have an indirect regulatory role on Vγ9Vδ2 T cells function might be of interest to study in both solid tumors and infected cells.

Until 2020, our knowledge on BTN2A1 functions did not involve Vγ9Vδ2 T cells, except for our publication in 2014 (Riaño et al., 2014) indicating that genetic elements located in chromosome 6 were mandatory for Vγ9Vδ2 TCR triggering. Most of the studies analyzing gene polymorphisms and genome-wide association studies (GWASs) indicated that BTN2A1 could be involved in multiple human diseases. Without being exhaustive, several compelling studies have suggested that BTN2A1 gene polymorphisms might be associated with multiple human diseases, including myocardial infarction, metabolic syndrome, hypertension, dyslipidemia, and hepatitis C (Yamada et al., 2011) (Ampuero et al., 2015; Fujimaki et al., 2011; Horibe et al., 2011; Murakata et al., 2014; Oguri et al., 2011). At present, although evidence is available on the involvement of Vγ9Vδ2 T cells in infectious diseases and cancer, their role in other human diseases is yet to be demonstrated. A careful study of BTN2A1 in these patient cohorts is important, and our anti-BTN2A1 mAbs could be valuable tools to provide a better understanding on the role of BTN2A1. Another consideration is the role of BTN2A1 in other cells types, including immune cells and somatic tissues. Currently, data on BTN2A1 protein expression are scarce, and although we have observed that in cancer patients T cells might express BTN2A1 (D.O., data not shown), a more comprehensive analysis of BTN2A1 expression in cancer and other pathologies is needed.

Our observations with BTN2A1 domain shuffling are consistent with nuclear magnetic resonance (NMR) data from Karunakaran et al. (2020) showing direct interaction of BTN2A1-V and BTN3A1-V domains, together with the knowledge of BTN2A1 interaction with the Vγ9 chain TCR, a model can be proposed. In this model, BTN2A1 would elicit the first contact between the target cell and Vγ9Vδ2 T cells, and drags along BTN3A1 to the immunological synapse, which in turn would transduce pAg signals from inside-out of the target cell to be exposed to the Vγ9Vδ2 T cells, hence activating them. However, in such a model there are several questions unsolved, including the existence and identity of the partner for BTN3A1 on the Vγ9Vδ2 T cell side. Moreover, Vantourout et al. (2009) showed that BTN3A2 was also essential for BTN3A1 export to the plasma membrane, and we found that BTN2A1 can also interact with BTN3A2 and BTN3A3. Hence, the actual composition and stoichiometry of BTN2A1- and BTN3A1-containing complexes at the plasma membrane, as well as the kinetics of the formations of such complexes during the immunological synapse between Vγ9Vδ2 T cells and target cells, remain to be elucidated.

We generated BTN2A1 mAbs displaying variable ability to prevent Vγ9Vδ2 T cell function against various tumor cell lines and primary leukemias. As was the case for anti-BTN3A 20.1 and 103.2 mAbs, once again mAbs proved to be valuable tools for addressing the cytotoxic function of Vγ9Vδ2 T cells. This is an important observation, since it will help understanding the mechanisms of recognition of different cancers, in addition to what we have already found in leukemias and pancreatic ductal adenocarcinoma (PDAC) (Benyamine et al., 2016, 2017). We will be able to tackle the mechanisms of recognition of cancer cells by Vγ9Vδ2 T cells and specifically the role of BTN2A1 in different tumor types. In addition, this will allow us to show whether BTN2A1 is readily present on the tumor cell surface in tissues.

The inhibitory effects of our anti-BTN2A1 mAbs are seen using either amino bisphosphonate or anti-BTN3A activating mAb. Hence, inhibitory anti-BTN2A1 mAbs alter these two different immune responses to both intracellular pAgs in tumor cells or direct triggering with agonistic anti-BTN3A 20.1 mAb. Based on the recent observations (Rigau et al., 2020), we tested different hypotheses. One hypothesis would be that the inhibitory anti-BTN2A1 mAbs prevent BTN2A1 interaction with the Vγ9 chain and consequently prevent Vγ9Vδ2 T cell activation. To test this hypothesis, we used soluble recombinant Vγ9Vδ2 TCR and assessed the eventual blocking effect of our mAbs on TCR binding to BTN2A1 at the membrane of BTN2A1-expressing cells. Our stronger antagonist anti-BTN2A1 mAb prevented Vγ9Vδ2 TCR binding. Another mechanism of action has been evoked for anti-BTN2A1 mAb activity involving the ability to disrupt BTN3A1/BTN2A1 complexes and consequently interfere with Vγ9Vδ2 T cell activation. Among our seven different anti-BTN2A1 mAbs, some were able to enhance BTN3A1/BTN2A1 interaction whereas others prevented it. Hence, although we cannot rule out that modulation of the interaction between BTN2A1 and BTN3A1 could impact Vγ9Vδ2 T cell activation, our data and recent studies indicate that other mechanisms might be at work. Hitherto, no ligand of BTN3A1 has been identified, although we have observed low-affinity binders of BTN3A1-Fc recombinant protein in various cells types (Compte et al., 2004; Vyborova et al., 2020), including Vγ9Vδ2 T cells (C.I., data not shown). We hypothesize that blocking anti-BTN2A1 mAbs might alter the binding of the BTN3A1/BTN2A1 complexes to a putative BTN3A1 ligand whether linked to the TCR or to another molecule. Herein, we have discussed the use of inhibiting BTN2A1 antibodies in an oncology setting as tools to understand the role of BTN2A1 in the Vγ9Vδ2 T cell anti-tumor response. For therapeutic applications, it would be interesting to investigate these inhibitory BTN2A1 antibodies in an

autoimmune setting, since Vγ9Vδ2 T cells have been reported to be dysregulated is several autoimmune diseases (Bank, 2020).

In summary, we have shown a complex set of interactions between BTN2A1 and BTN3A molecules, modulated by pAgs and critical for their exposure to the plasma membrane. We demonstrated the impact of these interactions on Vγ9Vδ2 T cell cytotoxicity against malignant cells, including primary human tumors, involving BTN2A1 but not BTN2A2. In addition, anti-BTN2A1 mAbs were generated that allowed us to understand the function of Vγ9Vδ2 T cells and the mechanism of action of their anti-tumor responses.

STAR★METHODS

Detailed methods are provided in the online version of this paper and include the following:

- KEY RESOURCES TABLE
- RESOURCE AVAILABILITY
  - Lead contact
  - Materials availability
  - Data and code availability
- EXPERIMENTAL MODEL AND SUBJECT DETAILS
  - Cell lines
  - Primary cell cultures
- METHOD DETAILS
  - Lentiviral transduction and CRISPR-Cas9-mediated BTN2A knockout
  - Co-immunoprecipitation and immunoblot analysis
  - Functional assay on Vγ9Vδ2 T cells
  - Quantification of BTN2A and BTN3A expression at the plasma membrane
  - Fluorescence resonance energy transfer (FRET) experiments
  - Proximity ligation assay (PLA)
  - Murine Vγ9Vδ2 TCR reporter assays
  - Anti-BTN2A1 mAb generation
  - Vγ9Vδ2 T cell cytotoxic activity using the Ishikawa spheroid model
  - Recombinant Vγ9Vδ2 TCR production and competitive binding assay
  - Assessments of antibody affinity toward BTN2A1
  - Epitope binning assays
  - Quantitative PCR
- QUANTIFICATION AND STATISTICAL ANALYSIS

SUPPLEMENTAL INFORMATION

Supplemental information can be found online at https://doi.org/10.1016/j.celrep.2021.109359.

ACKNOWLEDGMENTS

The D.O. and E.S. teams are labeled Equipe Fondation Recherche Médicale DEQ20180339209 and DEQ20170839118, respectively. D.O. is a Senior Scholar of the Institut Universitaire de France. This study was supported by SATT Sud-Est under the agreement 793-SA-16-AMU. We would like to thank Pierre Pontarotti for advice and manuscript editing and Isabel Gregoire, Tim Carlton, and Lena Daher for careful reading of the manuscript.

AUTHOR CONTRIBUTIONS

C.E.C., C.P., A.D.G., E.S., T.H., R.H., N.V., and D.O. designed the study/experiments. C.E.C., A.D.G., C.K., M.G., M.F., E.G., C.R., C.I., L.G., N.V., A.B., and A.C.I.F. performed experiments. C.E.C., C.P., A.D.G., and D.O. analyzed and interpreted the data. C.E.C. and D.O. wrote the manuscript. All authors critically reviewed the manuscript.

DECLARATION OF INTERESTS

D.O. is cofounder and shareholder of Imcheck Therapeutics. C.E.C., A.D.G., R.H., M.F., M.G., E.G., and C.K. are employees and shareholders of Imcheck Therapeutics. D.O. and C.P. are inventors of patent WO/2019/057933. The remaining authors declare no competing interests.

Received: April 3, 2020
Revised: August 27, 2020
Accepted: June 17, 2021
Published: July 13, 2021

REFERENCES

Adams, E.J., Gu, S., and Luoma, A.M. (2015). Human gamma delta T cells: Evolution and ligand recognition. Cell. Immunol. *296*, 31–40.

Allison, T.J., Winter, C.C., Fournié, J.J., Bonneville, M., and Garboczi, D.N. (2001). Structure of a human γδ T-cell antigen receptor. Nature *411*, 820–824.

Ammann, J.U., Cooke, A., and Trowsdale, J. (2013). Butyrophilin Btn2a2 inhibits TCR activation and phosphatidylinositol 3-kinase/Akt pathway signaling and induces Foxp3 expression in T lymphocytes. J. Immunol. *190*, 5030–5036.

Ampuero, J., del Campo, J.A., Rojas, L., García-Lozano, R.J., Buti, M., Solá, R., Forns, X., Moreno-Otero, R., Andrade, R., Diago, M., et al. (2015). Fine-mapping butyrophilin family genes revealed several polymorphisms influencing viral genotype selection in hepatitis C infection. Genes Immun. *16*, 297–300.

Amslinger, S., Hecht, S., Rohdich, F., Eisenreich, W., Adam, P., Bacher, A., and Bauer, S. (2007). Stimulation of Vγ9/Vδ2 T-lymphocyte proliferation by the isoprenoid precursor, (*E*)-1-hydroxy-2-methyl-but-2-enyl 4-diphosphate. Immunobiology *212*, 47–55.

Bank, I. (2020). The role of gamma delta T cells in autoimmune rheumatic diseases. Cells *9*, 462.

Banning, C., Votteler, J., Hoffmann, D., Koppensteiner, H., Warmer, M., Reimer, R., Kirchhoff, F., Schubert, U., Hauber, J., and Schindler, M. (2010). A flow cytometry-based FRET assay to identify and analyse protein-protein interactions in living cells. PLoS ONE *5*, e9344.

Benyamine, A., Le Roy, A., Mamessier, E., Gertner-Dardenne, J., Castanier, C., Orlanducci, F., Pouyet, L., Goubard, A., Collette, Y., Vey, N., et al. (2016). BTN3A molecules considerably improve Vγ9Vδ2T cells-based immunotherapy in acute myeloid leukemia. OncoImmunology *5*, e1146843.

Benyamine, A., Loncle, C., Foucher, E., Blazquez, J.-L., Castanier, C., Chrétien, A.-S., Modesti, M., Secq, V., Chouaib, S., Gironella, M., et al. (2017). BTN3A is a prognosis marker and a promising target for Vγ9Vδ2 T cells based-immunotherapy in pancreatic ductal adenocarcinoma (PDAC). OncoImmunology *7*, e1372080.

Blazquez, J.-L., Benyamine, A., Pasero, C., and Olive, D. (2018). New insights into the regulation of γδ T cells by BTN3A and other BTN/BTNL in tumor immunity. Front. Immunol. *9*, 1601.

Compte, E., Pontarotti, P., Collette, Y., Lopez, M., and Olive, D. (2004). Frontline: Characterization of BT3 molecules belonging to the B7 family expressed on immune cells. Eur. J. Immunol. *34*, 2089–2099.

Dustin, M.L., Scotet, E., and Olive, D. (2019). An X-ray vision for phosphoantigen recognition. Immunity *50*, 1026–1028.

Eberl, M., Hintz, M., Reichenberg, A., Kollas, A.-K., Wiesner, J., and Jomaa, H. (2003). Microbial isoprenoid biosynthesis and human γδ T cell activation. FEBS Lett. *544*, 4–10.

Fujimaki, T., Kato, K., Oguri, M., Yohida, T., Horibe, H., Yokoi, K., Watanabe, S., Satoh, K., Aoyagi, Y., Tanaka, M., et al. (2011). Association of a polymorphism of BTN2A1 with dyslipidemia in East Asian populations. Exp. Ther. Med. *2*, 745–749.

Gober, H.-J., Kistowska, M., Angman, L., Jenö, P., Mori, L., and De Libero, G. (2003). Human T cell receptor γδ cells recognize endogenous mevalonate metabolites in tumor cells. J. Exp. Med. *197*, 163–168.

Gu, S., Sachleben, J.R., Boughter, C.T., Nawrocka, W.I., Borowska, M.T., Tarrasch, J.T., Skiniotis, G., Roux, B., and Adams, E.J. (2017). Phosphoantigen-induced conformational change of butyrophilin 3A1 (BTN3A1) and its implication on Vγ9Vδ2 T cell activation. Proc. Natl. Acad. Sci. USA *114*, E7311–E7320.

Gu, S., Borowska, M.T., Boughter, C.T., and Adams, E.J. (2018). Butyrophilin3A proteins and Vγ9Vδ2 T cell activation. Semin. Cell Dev. Biol. *84*, 65–74.

Harly, C., Guillaume, Y., Nedellec, S., Peigné, C.-M., Mönkkönen, H., Mönkkönen, J., Li, J., Kuball, J., Adams, E.J., Netzer, S., et al. (2012). Key implication of CD277/butyrophilin-3 (BTN3A) in cellular stress sensing by a major human γδ T-cell subset. Blood *120*, 2269–2279.

Heuston, S., Begley, M., Gahan, C.G.M., and Hill, C. (2012). Isoprenoid biosynthesis in bacterial pathogens. Microbiology (Reading) *158*, 1389–1401.

Horibe, H., Kato, K., Oguri, M., Yoshida, T., Fujimaki, T., Kawamiya, T., Yokoi, K., Watanabe, S., Satoh, K., Aoyagi, Y., et al. (2011). Association of a polymorphism of BTN2A1 with hypertension in Japanese individuals. Am. J. Hypertens. *24*, 924–929.

Karunakaran, M.M., Göbel, T.W., Starick, L., Walter, L., and Herrmann, T. (2014). Vγ9 and Vδ2 T cell antigen receptor genes and butyrophilin 3 (*BTN3*) emerged with placental mammals and are concomitantly preserved in selected species like alpaca (*Vicugna pacos*). Immunogenetics *66*, 243–254.

Karunakaran, M.M., Willcox, C.R., Salim, M., Paletta, D., Fichtner, A.S., Noll, A., Starick, L., Nöhren, A., Begley, C.R., Berwick, K.A., et al. (2020). Butyrophilin-2A1 directly binds germline-encoded regions of the Vγ9Vδ2 TCR and is essential for phosphoantigen sensing. Immunity *52*, 487–498.e6.

Li, J., Herold, M.J., Kimmel, B., Müller, I., Rincon-Orozco, B., Kunzmann, V., and Herrmann, T. (2009). Reduced expression of the mevalonate pathway enzyme farnesyl pyrophosphate synthase unveils recognition of tumor cells by Vγ9Vδ2 T cells. J. Immunol. *182*, 8118–8124.

Morita, C.T., Beckman, E.M., Bukowski, J.F., Tanaka, Y., Band, H., Bloom, B.R., Golan, D.E., and Brenner, M.B. (1995). Direct presentation of nonpeptide prenyl pyrophosphate antigens to human γδ T cells. Immunity *3*, 495–507.

Morita, C.T., Jin, C., Sarikonda, G., and Wang, H. (2007). Nonpeptide antigens, presentation mechanisms, and immunological memory of human Vγ2Vδ2 T cells: Discriminating friend from foe through the recognition of prenyl pyrophosphate antigens. Immunol. Rev. *215*, 59–76.

Murakata, Y., Fujimaki, T., and Yamada, Y. (2014). Association of a butyrophilin, subfamily 2, member A1 gene polymorphism with hypertension. Biomed. Rep. *2*, 818–822.

Oguri, M., Kato, K., Yoshida, T., Fujimaki, T., Horibe, H., Yokoi, K., Watanabe, S., Satoh, K., Aoyagi, Y., Tanaka, M., et al. (2011). Association of a genetic variant of BTN2A1 with metabolic syndrome in East Asian populations. J. Med. Genet. *48*, 787–792.

Palakodeti, A., Sandstrom, A., Sundaresan, L., Harly, C., Nedellec, S., Olive, D., Scotet, E., Bonneville, M., and Adams, E.J. (2012). The molecular basis for modulation of human Vγ9Vδ2 T cell responses by CD277/butyrophilin-3 (BTN3A)-specific antibodies. J. Biol. Chem. *287*, 32780–32790.

Peigné, C.-M., Léger, A., Gesnel, M.-C., Konczak, F., Olive, D., Bonneville, M., Breathnach, R., and Scotet, E. (2017). The juxtamembrane domain of butyrophilin BTN3A1 controls phosphoantigen-mediated activation of human Vγ9Vδ2 T cells. J. Immunol. *198*, 4228–4234.

Rhodes, D.A., Stammers, M., Malcherek, G., Beck, S., and Trowsdale, J. (2001). The cluster of *BTN* genes in the extended major histocompatibility complex. Genomics *71*, 351–362.

Riaño, F., Karunakaran, M.M., Starick, L., Li, J., Scholz, C.J., Kunzmann, V., Olive, D., Amslinger, S., and Herrmann, T. (2014). Vγ9Vδ2 TCR-activation by phosphorylated antigens requires butyrophilin 3 A1 (*BTN3A1*) and additional genes on human chromosome 6. Eur. J. Immunol. *44*, 2571–2576.

Rigau, M., Ostrouska, S., Fulford, T.S., Johnson, D.N., Woods, K., Ruan, Z., McWilliam, H.E.G., Hudson, C., Tutuka, C., Wheatley, A.K., et al. (2020). Butyrophilin 2A1 is essential for phosphoantigen reactivity by γδ T cells. Science *367*, eaay5516.

Sandstrom, A., Peigné, C.-M., Léger, A., Crooks, J.E., Konczak, F., Gesnel, M.-C., Breathnach, R., Bonneville, M., Scotet, E., and Adams, E.J. (2014). The intracellular B30.2 domain of butyrophilin 3A1 binds phosphoantigens to mediate activation of human Vγ9Vδ2 T cells. Immunity *40*, 490–500.

Sarter, K., Leimgruber, E., Gobet, F., Agrawal, V., Dunand-Sauthier, I., Barras, E., Mastelic-Gavillet, B., Kamath, A., Fontannaz, P., Guéry, L., et al. (2016). Btn2a2, a T cell immunomodulatory molecule coregulated with MHC class II genes. J. Exp. Med. *213*, 177–187.

Smith, I.A., Knezevic, B.R., Ammann, J.U., Rhodes, D.A., Aw, D., Palmer, D.B., Mather, I.H., and Trowsdale, J. (2010). BTN1A1, the mammary gland butyrophilin, and BTN2A2 are both inhibitors of T cell activation. J. Immunol. *184*, 3514–3525.

Starick, L., Riano, F., Karunakaran, M.M., Kunzmann, V., Li, J., Kreiss, M., Amslinger, S., Scotet, E., Olive, D., De Libero, G., and Herrmann, T. (2017). Butyrophilin 3A (BTN3A, CD277)-specific antibody 20.1 differentially activates Vγ9Vδ2 TCR clonotypes and interferes with phosphoantigen activation. Eur. J. Immunol. *47*, 982–992.

Tanaka, Y., Morita, C.T., Tanaka, Y., Nieves, E., Brenner, M.B., and Bloom, B.R. (1995). Natural and synthetic non-peptide antigens recognized by human γδ T cells. Nature *375*, 155–158.

Thompson, K., Rojas-Navea, J., and Rogers, M.J. (2006). Alkylamines cause Vγ9Vδ2 T-cell activation and proliferation by inhibiting the mevalonate pathway. Blood *107*, 651–654.

Vantourout, P., Mookerjee-Basu, J., Rolland, C., Pont, F., Martin, H., Davrinche, C., Martinez, L.O., Perret, B., Collet, X., Périgaud, C., et al. (2009). Specific requirements for Vγ9Vδ2 T cell stimulation by a natural adenylated phosphoantigen. J. Immunol. *183*, 3848–3857.

Vantourout, P., Laing, A., Woodward, M.J., Zlatareva, I., Apolonia, L., Jones, A.W., Snijders, A.P., Malim, M.H., and Hayday, A.C. (2018). Heteromeric interactions regulate butyrophilin (BTN) and BTN-like molecules governing γδ T cell biology. Proc. Natl. Acad. Sci. USA *115*, 1039–1044.

Vyborova, A., Beringer, D.X., Fasci, D., Karaiskaki, F., van Diest, E., Kramer, L., de Haas, A., Sanders, J., Janssen, A., Straetemans, T., et al. (2020). γ9δ2T cell diversity and the receptor interface with tumor cells. J. Clin. Invest. *130*, 4637–4651.

Wang, H., Fang, Z., and Morita, C.T. (2010). Vγ2Vδ2 T cell receptor recognition of prenyl pyrophosphates is dependent on all CDRs. J. Immunol. *184*, 6209–6222.

Wang, H., Nada, M.H., Tanaka, Y., Sakuraba, S., and Morita, C.T. (2019). Critical roles for coiled-coil dimers of butyrophilin 3A1 in the sensing of prenyl pyrophosphates by human Vγ2Vδ2 T cells. J. Immunol. *203*, 607–626.

Yamada, Y., Nishida, T., Ichihara, S., Sawabe, M., Fuku, N., Nishigaki, Y., Aoyagi, Y., Tanaka, M., Fujiwara, Y., Yoshida, H., et al. (2011). Association of a polymorphism of BTN2A1 with myocardial infarction in East Asian populations. Atherosclerosis *215*, 145–152.

Yang, Y., Li, L., Yuan, L., Zhou, X., Duan, J., Xiao, H., Cai, N., Han, S., Ma, X., Liu, W., et al. (2019). A structural change in butyrophilin upon phosphoantigen binding underlies phosphoantigen-mediated Vγ9Vδ2 T cell activation. Immunity *50*, 1043–1053.e5.

STAR★METHODS

KEY RESOURCES TABLE

REAGENT or RESOURCE	SOURCE	IDENTIFIER
Antibodies		
Mouse c-myc 9E10	Invitrogen	Cat#MA1-980
anti-GFP antibody	Sigma Aldrich	Cat#11814460001; RRID:AB_390913
anti-BTN2A mAb (clones 7.48, 7.28, 8.15, 8.16, 4.15, 5.28 and 8.33)	PCT/EP2018/075689	N/A
Anti-CD107(a)	BD biosciences	Cat#560949; RRID:AB_396134
Anti-CD107(b)	BD biosciences	Cat#555804; RRID:AB_396138
Rabbit anti-flag	Sigma Aldrich	Cat#Millipore F7425; RRID:AB_439687
anti-BTN3A1 20.1 mAb	UMR 599 INSERM, Centre de Recherche en Cancérologie de Marseille. (Compte et al., 2004)	N/A
anti-BTN3A1 103.2 mAb	UMR 599 INSERM, Centre de Recherche en Cancérologie de Marseille. (Compte et al., 2004)	N/A
PE Fab'2 Goat anti Human IgG (H+L)	Jackson Immunoresearch	Cat#109-116-088; RRID: AB_2337676
anti-human Fc-HRP	Biorad	Cat#AHP1323P; RRID AB_877442
anti-His-HRP	Biorad	Cat#MA1-135; RRID: AB_2610638
Mouse anti-human CD107a IGG1	BD BIOSCIENCES	Cat# 555800; batch 9311781; clone H4A3; RRID:AB_396134
Mouse anti-human anti-CD107b IGG1	BD BIOSCIENCES	Cat# 555804; batch 9207143; clone H4B4; RRID:AB_396138
Cytofix/Cytoperm	BD BIOSCIENCES	Cat# 554714
Mouse anti-human anti-perforin IGG2B	BD BIOSCIENCES	Cat#563764; clone δG9; RRID:AB_2738411
Mouse anti-human anti-granzyme B IGG1	BD BIOSCIENCES	Cat# 566996; clone 4B2G4; RRID:AB_2869996
Mouse anti-human IFNγ IGG1	MILTENYI BIOTEC	Cat# 130-113-493; RRID: AB_2733589
Mouse anti-human TNFα IGG1	MILTENYI BIOTEC	Cat# 130-118-974; RRID: AB_2751595
Mouse anti-human IGG1	MILTENYI BIOTEC	Cat# 130-106-545; RRID: AB_2733683
Mouse anti-human CD3 IGG1	BECKMAN COULTER	Cat#B49204; batch 200030; clone UCHT1
Mouse anti-human TCR Vδ2 IGG1	BIOLEGEND	Cat#331422; batch B281873; clone B6; RRID: AB_2687328
Biological samples		
Blood samples from healthy volunteers	Local Blood Bank-*Etablissement Français du Sang* (EFS)-Marseille-France	https://dondesang.efs.sante.fr/
Blood samples from acute myeloid leukemia patients	Institut Paoli Calmettes, Marseille, France	https://www.institutpaolicalmettes.fr/
Chemicals, peptides, and recombinant proteins		
Recombinant human IL-2	Novartis (Proleukin)	N/A
Zoledronic acid monohydrate	Sigma Aldrich	SML0223; CAS: 165800-06-6
Phorbol 12-myristate 13-acetate	Sigma Aldrich	Cat#P8139-1MG
Ionomycine	Sigma Aldrich	Cat#I0634-1MG
HMBPP	Sigma Aldrich	Cat#95098
BTN2A1-Fc fusion protein	R&D Systems	Cat# 9058-BT
AF647 labeling kit	ThermoFisher Scientific	Cat# A20186
DSB-X Biotin Protein Labeling Kit	ThermoFisher Scientific	Cat# D20655
Recombinant human BTN2A1-His protein	R&D Systems	Cat#9058-BT-050

(*Continued on next page*)

Continued

REAGENT or RESOURCE	SOURCE	IDENTIFIER
Critical commercial assays		
LentiX concentrator	Takara Bio	Cat#631232
Pierce BCA Protein Assay Kit	ThermoFisher Scientific	Cat# 23225
Protein G chromatography column	GE Healthcare	Cat#17-0618-01
GolgiStop protein transport inhibitor	BD BIOSCIENCES	Cat# 554724
CellQuant calibrator kit	Biocytex	Cat# 7208
Duolink kit PLA	Sigma Aldrich	Cat# DUO92007
Mouse IL-2 ELISA kit	Invitrogen	Cat#88-7024-88
CellTrace Violet	Invitrogen	Cat#C34557
CellEvent Caspase-3/7 Reagent green	Invitrogen	Cat#C10423
Protein A chromatography column	GE Healthcare	GE17-0402-01
Cell Proliferation Dye eFluor 670	ThermoFisher Scientific	Cat# 65-0840-90
CellEvent caspase −3/7 Green	ThermoFisher Scientific	Cat# C10423
Experimental models: Cell lines		
HL-60 (promyelocytic leukemia)	ATCC	ATCC® CCL-240
Raji (Burkitt's lymphoma)	ATCC	ATCC® CCL-86
Daudi (B lymphoblast)	ATCC	ATCC® CCL-213
K562 (chronic myelogenous leukemia)	ATCC	ATCC® CCL-243
HCT116 (colorectal carcinoma)	ATCC	ATCC® CCL-247
PC3 (prostate adenocarcinoma)	ATCC	ATCC® CRL-1435
Panc-1 (pancreas adenocarcinoma)	ATCC	ATCC® CRL-1469
MDA-MB-231 (breast carcinoma)	ATCC	ATCC® HTB-26
HEK293T (human embryonic kidney)	ATCC	ATCC® CRL-1573
A549 (lung adenocarcinoma)	ATCC	ATCC® CCL-185
Mouse fibroblast cell line NIH 3T3	ATCC	ATCC® CRL-1658
53/4 hybridoma cells expressing the human Vγ9Vδ2 TCR	INSERM UMR 599, UniversitédelaMé diterrané e, Cancer and Immunology Institute of Marseille, IFR 137, Marseille, France INSERM UMR 599, UniversitédelaMé diterrané e, Cancer and Immunology Institute of Marseille, IFR 137, Marseille, France (Starick et al., 2017)	N/A
HEK293T BTN2AKO	This manuscript	N/A
HEK293T BTN2AKO/BTN3AKO	This manuscript	N/A
HEK293T BTN2AKO +2A1	This manuscript	N/A
HEK293T BTN2AKO +2A2	This manuscript	N/A
HEK293T BTN2AKO/BTN3AKO +2A1	This manuscript	N/A
HEK293T BTN2AKO/BTN3AKO +3A1	This manuscript	N/A
HEK293T BTN2AKO/BTN3AKO +3A2	This manuscript	N/A
HEK293T BTN2AKO/BTN3AKO +3A3	This manuscript	N/A
HEK293T BTN2AKO/BTN3AKO +2A1+3A1	This manuscript	N/A
HEK293T BTN2AKO/BTN3AKO +2A1+3A2	This manuscript	N/A
HEK293T BTN2AKO/BTN3AKO +2A1+3A3	This manuscript	N/A
Ishikawa endometrial adenocarcinoma cell line	Dr. J. Downward laboratory at the Francis Crick Institute	N/A
Chinese hamster ovary cells	ECACC	85050302
Recombinant Vγ9Vδ2 TCR (clone G115,) with a C-terminal Fc-tag on the Vγ9 chain	This manuscript	N/A

(*Continued on next page*)

Continued

REAGENT or RESOURCE	SOURCE	IDENTIFIER
Oligonucleotides		
TaqManAssay_BTN3A1 Probe	ThermoFisher Scientific	Hs01063368_m1
TaqManAssay_BTN3A2 Probe	ThermoFisher Scientific	Hs00389328_m1
TaqManAssay_BTN3A3 Probe	ThermoFisher Scientific	Hs00757230_m1
TaqManAssay_TBP Probe	ThermoFisher Scientific	Hs00427620_m1
Recombinant DNA		
lentiCRISPR-v2 vector	Addgene	RRID: Addgene_52961
pMD2.G expression vector	Addgene	RRID: Addgene_12259
psPAX2 expression vector	Addgene	RRID: Addgene_12260
pLV-EF1α-puro vector	Custom DNA Constructs	N/A
BTN2A guide 44 lentiviral vector (BTN2A1/A2 (exon3) specific sgRNA CACCGACA GTGTGGAGGGACCCCTA	This manuscript	N/A
pcDNA3.1_eCFP-eYFP (eCFP-YFP fusion cloned BamH1/Not1 into pcDNA3.1-Zeo)	Custom, GeneArt	N/A
pcDNA3.1_eCFP	Custom, GeneArt	N/A
pcDNA3.1_eYFP	Custom, GeneArt	N/A
pLV-BTN2A1-myc	Custom, GeneArt	N/A
pcDNA3.1_BTN3A1_link_eYFP	Custom, GeneArt	N/A
pcDNA3.1_BTN3A1_link_eCFP	Custom, GeneArt	N/A
pcDNA3.1_BTN3A1_link_eGFP	Custom, GeneArt	N/A
pcDNA3.1-BTN3A1_DeltaB30.2_YFP	Custom, GeneArt	N/A
pcDNA3.1_BTN3A2_link_eYFP	Custom, GeneArt	N/A
pcDNA3.1_BTN3A2_link_eCFP	Custom, GeneArt	N/A
pcDNA3.1_BTN3A3_link_eYFP	Custom, GeneArt	N/A
pcDNA3.1_BTN3A3_link_eCFP	Custom, GeneArt	N/A
pcDNA3.1_BTN2A1_link_eYFP	Custom, GeneArt	N/A
pcDNA3.1_BTN2A1_link_eCFP	Custom, GeneArt	N/A
pcDNA3.1_BTN2A1_deltaB30.2_eCFP	Custom, GeneArt	N/A
pcDNA3.1_BTN2A1_JTM-BTLA_eCFP	Custom, GeneArt	N/A
pcDNA3.1_BTN2A1_EC-BTLA_eCFP	Custom, GeneArt	N/A
pcDNA3.1_BTN2A1_JTM-BTLA_eCFP	Custom, GeneArt	N/A
pcDNA3.1_BTN2A2_link_eYFP	Custom, GeneArt	N/A
pcDNA3.1_BTN2A2_link_eCFP	Custom, GeneArt	N/A
pcDNA3.1_BTN2A1_JTM-BTN2A2_eCFP	Custom, GeneArt	N/A
pcDNA3.1_BTN2A2_deltaB30.2_eYFP	Custom, GeneArt	N/A
pcDNA3.1_BTN2A2_JTM-BTLA_eYFP	Custom, GeneArt	N/A
pcDNA3.1_BTN2A2_JTM-BTN2A1_eYFP	Custom, GeneArt	N/A
pcDNA3.1_BTN2A2_JTM-BTLA_eYFP	Custom, GeneArt	N/A
pcDNA3.1_BTN2A2_EC-BTLA_eYFP	Custom, GeneArt	N/A
pLV-BTN2A1-wt (BTN2A1 optimized from …	Custom, GeneArt	N/A
pLV-BTN2A2-wt	Custom, GeneArt	N/A
pLenti_BTN3A1-MycDDK	Origene	RC216344L3
pLenti_BTN3A2-MycDDK	Origene	RC201183L3
pLenti_BTN3A3-MycDDK	Origene	RC220673
Software and algorithms		
FlowJo 10.5.3 software	FlowJo LLC	https://www.flowjo.com/solutions/flowjo
ImageJ	ImageJ	https://imagej.net/

(*Continued on next page*)

Continued

REAGENT or RESOURCE	SOURCE	IDENTIFIER
GraphPad Prism 8.0.1	GraphPad Inc	https://www.graphpad.com/scientific-software/prism/
Other		
Turbofect reagent	ThermoFisher Scientific	Cat#R0531
TaqMan Fast Advanced Master Mix	ThermoFisher Scientific	4444557
Hoechst 33342	ThermoFisher Scientific	Cat#H3570
LIVE/DEAD fixable aqua dead cell stain	ThermoFisher Scientific	Cat# L34966

RESOURCE AVAILABILITY

Lead contact

Further information and requests for resources and reagents should be directed to and will be fulfilled by the Lead contact, Carla Cano (carla.cano@imcheck.fr)

Materials availability

All anti-BTN2A antibodies generated in this study are available from the Lead Contact with a completed Materials Transfer Agreement.

Data and code availability

- All data reported in this paper will be shared by the lead contact upon request.
- This study did not generate any unique code.
- Any additional information required to reanalyze the data reported in this paper is available from the lead contact upon request

EXPERIMENTAL MODEL AND SUBJECT DETAILS

Cell lines

HL-60 (promyelocytic leukemia), Raji (Burkitt's lymphoma), Daudi (B lymphoblast) and K562 (chronic myelogenous leukemia) cells were cultured in RPMI 1640 Glutamax medium supplemented with 10% fetal bovine serum (FBS), 1% Na-Pyruvate. HCT116 (colorectal carcinoma) were cultured in McCoy's medium supplemented with 10% FBS, 1% Na-Pyruvate. PC3 (prostate adenocarcinoma), Panc-1 (pancreas adenocarcinoma), MDA-MB-231 (breast carcinoma), HEK293T (human embryonic kidney) and its derivatives were cultured in DMEM Glutamax medium supplemented with 10% FBS, 1% Na-Pyruvate. A549 (lung adenocarcinoma) cells were cultured in Ham's F12/Kaighn's 10% FCS, 1% Na-Pyruvate. The Ishikawa endometrial adenocarcinoma cell line was kindly provided by Dr. J. Downward laboratory at the Francis Crick Institute and cultured according to their recommendations. 53/4 hybridoma cells expressing the human Vγ9Vδ2 TCR were kindly provided by the research group of Professor Dr. Thomas Herrmann- Institute of Virology and Immunobiology- University of Würzburg and prepared as previously described (Starick et al., 2017).

Primary cell cultures

Peripheral blood mononuclear cells (PBMCs) were obtained by centrifugation on density gradient (Eurobio) of whole blood from healthy volunteers (HV) provided by the local Blood Bank (Etablissement Français du Sang (EFS)).

Heparinized blood from 12 acute myeloid leukemia (AML) patients (8 men and 4 women) were obtained from the Department of Hematology (PI Pr. N. Vey, Institut Paoli Calmettes, Marseille, France). The patient's age ranged between 31 and 90 years (mean age ± SD: 58,8 ± 16,7 years). Under the French-American-British (FAB) classification patients belonged to subtypes M1 to M6 as follows: 3 patients to subtype M1, one patient to subtype M2, 3 patients to subtype M4, 4 patients to subtype M5 and one patient to subtype M6. Written informed consent was obtained from all donors in accordance with the Declaration of Helsinki, and the research was approved by the local institutional review boards of the Institut Paoli Calmettes (N° ID IPC1996).

All cell culture media were obtained from Life Technologies.

METHOD DETAILS

Lentiviral transduction and CRISPR-Cas9-mediated BTN2A knockout

For generation of lentiviral particles, HEK293T cells were transfected with pMD2.G, psPAX2 and pLV lentiviral expression vector, which was either empty or encoding the indicated gene of interest, using TurboFect reagent (ThermoFisher) according to

manufacturer's instructions. Transfection medium was replaced by OptiMEM™ (ThermoFisher) after 24h. Culture supernatant containing lentiviral particles was collected after 24 hr and 48 hr, and concentrated LentiX concentrator (Takara) following manufacturer's instructions. For HEK-BTN2A overexpressing transductants, wild-type human BTN2A1 or BTN2A2 were cloned into pLV-EF1α-puro vector using BamHI/SalI restriction sites. For all transductions, HEK293T cells were seeded in 12-wells plates ($2.5x10^5$ cells/well), and 25 μL of concentrated lentiviral particles were added to the culture. After 24 hr, cells were washed twice in complete medium, and cultured in their regular culture medium for 48 hr. For BTN2A gene inactivation, optimized CRISPR target sequences targeting both BTN2A isoforms (guide 44, sequence available upon request) were cloned into the lentiCRISPR-v2 vector (Addgene #52961). BTN2AKO cells were obtained by transduction of the indicated cell lines with the above-mentioned lentiviral guide 44 vector. BTN2AKO/3AKO HEK293T cells were obtained by transducing HEK293T BTN3AKO (described in Blazquez et al. manuscript in preparation) with BTN2A guide 44 lentiviral vector. For selection of HEK293T transductants, 1 μg/mL puromycin was added to the culture medium.

Co-immunoprecipitation and immunoblot analysis

BTN2AKO/BTN3AKO HEK293T cells were co-transfected with with pcDNA3-Zeo vectors encoding BTN3A1-GFP, BTN2A1-myc or BTN3A1-GFP + BTN2A1-myc using Lipofectamine 2000 from Thermofisher® in OptiMEM medium from GIBCO® according to manufacturer's instructions. After 48 hr, cells were lysed in 50mM Tris 1M pH 7.4, 150mM NaCl,5mM EDTA, 1% NP-40, 1%, containing protease inhibitors cocktail (MERCK®). After centrifugation 10 min at 13.000 rpm at 4°C, protein content in lysate supernatants were quantified using Pierce BCA Protein Assay Kit (ThermoFisher). Samples were brought to a concentration of 1 μg/μL in lysis buffer, and then incubated with the indicated antibodies overnight at 4°C. Next day, immunocomplexes were captured on protein G (GE Healthcare) for 45 minutes on rotary shaker at 4°C. Beads were washed five times in lysis buffer, and proteins were eluted in 4 × laemmli buffer (Biorad) with β-Mercaptoethanol (Euromedex) for 5 minutes at 95°C and on an 4%–15% SDS-PAGE (Biorad), before Western Bloting with the indicated mAbs. Mouse c-*myc* 9E10 was from Invitrogen® and anti-GFP antibody from ROCHE®. Whole cell lysates (input) were used to check for transfection efficiency.

Functional assay on Vγ9Vδ2 T cells

Purified Vγ9Vδ2 T cells from expanded healthy volunteers PBMCs (in presence of 1 μg/mL zoledronate, 200 UI/mL rhIL-2 for 12-14 days) and cultured overnight in rhIL-2 (200 UI/mL) prior to stimulation. Then, Vγ9Vδ2 T cells were co-cultured at 37°C with the indicated target cell lines (effector: target (E:T) ratio 1:1) with or without 10 μg/mL purified anti-BTN2A1 mAb or 1 or 10 μg/mL 20.1, or Zoledronate (10 μM), as indicated. Phorbol 12-myristate 13-acetate (PMA, 20 ng/mL) with ionomycine (1 μg/mL) were used as positive control for Vγ9Vδ2 T cell activation. Vγ9Vδ2 T cell degranulation was assessed after 4 hr incubation in presence of GolgiStop (BD Biosciences) and soluble CD107(a+b)-FITC. For assessment of perforin/granzyme B release, experiment was performed in the absence of GolgiStop. After 4 hr, cells were collected, fixed in PBS 2% paraformaldehyde and analyzed on a CytoFlex LX (Beckman Coulter) using FlowJo 10.5.3 software (FlowJo). Degranulation was determined by the percentage of CD107ab + cells among Vδ2 T cells (defined as CD3+ Panγδ TCR+).

Quantification of BTN2A and BTN3A expression at the plasma membrane

The number of BTN2A and BTN3A molecules displayed at the plasma membrane of the indicated cells was assessed using the CellQuant calibrator kit (Biocytex) according to manufacturer's instructions. Briefly, cells were stained with primary antibodies (10 μg/mL or as indicated otherwise) for 30 min at 4°C, with or without permeabilization using CytoFix/Cytoperm kit according to manufacturer's instructions (BD Biosciences), then staining was detected using PE-conjugated goat anti-mouse probe (Jackson Immunoresearch), which was previously incubated with CellQuant beads. Cells were fixed using Cytofix (BD Bioscience) and analyzed by flow cytometry (Cytoflex S, Beckman Coulter). Bead counts were analyzed by linear regression to obtain a calibration curve, depicting mean fluorescence intensity (MFI) correlation to the number of molecules displayed at the plasma membrane. Ratio between extracellular/intracellular number of molecules was calculated as an indicator of plasma membrane export. For evaluating the eventual correlation between BTN expression in target cells and Vγ9Vδ2 T cell degranulation, BTN quantification and degranulation assays were run simultaneously. Results were analyzed with linear regression between the percentage of CD107ab+ cells and the number of BTN molecules. Pearson correlation test was calculated for each graph. To merge results from two independent experiments, K562 cells were assessed twice and used as « reference cell line » for normalization (results for K562 cells were considered equal to 1). Then, results for each cell line was compared to K562 using « Cell / K562 value ».

Fluorescence resonance energy transfer (FRET) experiments

For eCFP or eYFP constructs, cDNA was synthesized (GeneArt) and cloned into pCDN3.1-Zeo+ backbone (Invitrogen™). A 39 aa linker was included between BTN3A/2A C-terminal end and -eXFP molecule in order to provide with flexibility and not interfere with molecule function. The reference sequence for BTN3A1 was the NM_007048, for BTN3A2, the reference coding sequence was the NM_001197246 and NM_006994 for BTN3A3. For BTN2A1 and BTN2A2, the reference sequences were NM_007049.5 and NM_006995.5 respectively. eCFP-eYFP fusion protein sequences (eCFP linked to eYFP by a 14 aa linker) were kindly provided by Pascal Schneider and Cristian Smulski (Lausanne; Switzerland). HEK293T cells were transiently transfected with eCFP and eYFP fusion proteins using lipofectamine 2000 reagent (Invitrogen™) according to manufacturer's instruction and analyzed by Flow

Cytometry 20–24 h post-transfection using a MacsQuant VYB Analyzer (Miltenyi™) or CytoFLEX (Beckman Coulter). eYFP signal was recorded using the 488 nm laser with a 525/50 filter, eCFP signal was recorded using the 405 nm laser with a 450/50 filter and FRET signal was recorded using the 405 nm laser with a 525/50 filter. Careful removal of background signals in the FRET channel is achieved using a FRET gate whose shape is function of the eYFP to eCFP ratio. Co-transfection of equal amounts of eCFP and eYFP is used to establish the background FRET levels whereas transfection of an eCFP–eYFP fusion protein serves to define FRET-positive cells according to Banning et al. (Banning et al., 2010). Signals obtained in the FRET channel with the experimental sample can, therefore, only be interpreted as bona fide FRET for cells expressing equal amount of the eYFP- and eCFP-fusion partners (i.e., for cells falling into gate of ratio 1:1). To achieve this, for each combination tested, plasmid DNA were titrated in order to determine the DNA quantity leading to 1:1 protein expression. For shuffling experiments, reference wild-type sequences of BTN2A1, BTN2A2 and BTN3A1 cDNAs were analyzed using InterProScan protein analysis tool (EMBL-EBI, UK) in order to identify the B30.2, transmembrane (TM) and ectodomain (EC) of each protein. Juxtamembrane (JTM) region was defined as the sequence between the end of the TM region and the DVVLD, which was considered as the equivalent of the DVILD motif in BTN3A1(Peigné et al., 2017). In all shuffled constructs but the DB30.2 (in which the whole B30.2 domain was deleted), the indicated domains were replaced by their equivalent in the BTLA cDNA. All BTN2A1 shuffled constructs contained a C-terminal linker followed by eCFP, whereas all BTN2A2 and BTN3A1 shuffled constructs bared C-terminal linker followed by eYFP. Sequences are available upon request. For assessment of the impact of anti-BTN2A mAbs on BTN2A1/BTN3A1 complex, cells were transfected concomitantly with BTN2A1-eCFP and BTN3A1-eYFP and treated with cycloheximide (10 μg/mL, Sigma) and bafilomycin A1 (0.1 μM, Invivogen) for 6 hr, then incubated with the indicated concentrations of anti-BTN2A and anti-BTN3A mAbs.

Proximity ligation assay (PLA)

HEK293T cells were co-transfected with plasmids encoding BTN2A1-myc and BTN3A1-flag using the JetPEI (Polyplus, Illkirch, France). After 36h, cells were plated on Ibidi® μ-Slide 8 well previously coated with human fibronectin (MerkTM, Darmstadt, Germany). Cells were then treated with 30 μM zoledronate overnight. Cells were fixed in 4% paraformaldehyde (Electron Microscopy Sciences, Hatfield, PA) for 10 minutes at RT, then permeabilized using permeabilization buffer (eBioscience). BTN2A1 and BTN3A1 were labeled with a mouse anti-myc (eBioscience, clone 9E10) and a rabbit anti-flag (Abcam), respectively. PLA was performed by using the Duolink kit according to manufacturer's instructions (Sigma), using the MINUS Mouse and PLUS Rabbit components. PLA signals were then revealed using Duolink *in situ* detection reagents orange. Hoechst 33342 (ThermoFisher) was added to the wells to stain nuclei. Imaging was performed with a Nikon A1, 60x objective, N.A 1.4 (Nikon®, Minato-ku, Tokyo, Japan) and their analysis was performed with ImageJ software as follow: nuclei and PLA signal spots were counted per image using the spot detector function. The number of PLA signal spots / number of nuclei was calculated for each image.

Murine Vγ9Vδ2 TCR reporter assays

Vγ9Vδ2 TCR (MOP) expressing 53/4 hybridoma cells were generated as reported earlier (Li et al., 2009; Starick et al., 2017). For assessment of the ability BTN2A isoforms to allow Vγ9Vδ2 TCR responsiveness in a fully murine setting, the mouse fibroblast cell line NIH 3T3 was transiently transfected with the indicated eCFP and eYFP fusion BTN3A and BTN2A isoforms using Lipofectamine LTX & PLUS Reagent kit (Invitrogen™) according to manufacturer's instructions. After 24 hr, 10^5 transfected cells were analyzed by flow cytometry for BTN3A and BTN2A expression. Then, $5x10^4$ transfected NIH 3T3 cells were co-cultured with $5x10^4$ 53/4 Vγ9Vδ2 TCR MOP reporter cells overnight, in presence of indicated stimuli (10 μM HMBPP, 10 μg/mL 20.1 or 103.2 mAb). In all experiments, Raji cells co-cultured with 53/4 hybridoma cells expressing the human MOP Vγ9Vδ2 TCR in presence of 10μM HMBPP, 10 μM or 100 μM Zoledronate were used as positive control (data not shown). 53/4 Vγ9Vδ2 TCR MOP reporter cells activation was measured by quantitation of mouse IL-2 secreted in co-culture supernatants by ELISA (Invitrogen #88-7024-88) as per manufacturer's protocol.

Anti-BTN2A1 mAb generation

Mouse anti-human BTN2A1 antibodies were generated by mouse immunization using recombinant human BTN2A1-Fc fusion protein (R&D Systems). Mice were bled after 21 days and mice displaying the highest BTN2A1-specific antibodies titer were euthanized. Splenic B cells were isolated via positive selection and underwent PEG-induced fusion to myeloma cells for hybridoma generation and cloned in HAT. Anti-BTN2A1 clones 7.48, 7.28, 8.15, 8.16, 4.15, 5.28 and 8.33 were described in patent PCT/EP2018/075689. VH and VL sequences of 8.15 and 8.16 were identical (data not shown).

Vγ9Vδ2 T cell cytotoxic activity using the Ishikawa spheroid model

To form spheroids, 3x104 Ishikawa cells were plated in low-attachment U-bottom plates (Costar) in cell culture media containing 10% Fetal Bovine Serum (FBS). Cells were incubated for 7 days at 37°C and 5% $C0_2$. Spheroids were then used for functional assay. To discriminate expanded Vγ9Vδ2 T cells from Ishikawa cells, Vγ9Vδ2 T cells from 4 different donors were stained using CellTrace Violet (Invitrogen) according to the manufacturer's instructions. $2x10^4$ Vγ9Vδ2 T cells were added to the spheroid culture following different conditions: spheroids alone, γδT cells, γδT cells + IgG1 isotype (10 μg/mL), γδT cells + anti-BTN3A1 20.1 mAb (10 μg/mL), γδT cells + anti-BTN2A1 7.48 mAb (10 μg/mL) or γδT cells + 20.1 + 7.48 mAbs. Spheroids and Vγ9Vδ2 T cells were co-cultured overnight in the presence of CellEvent Caspase-3/7 Reagent green (4 μM), a dye labeling apoptotic cells. Spheroids and Vγ9Vδ2 T cells were then dissociated by pipetting to obtain a suspension of cells. Caspase 3/7 positivity was then assessed by flow cytometry

(FACS Canto II, Becton Dickinson, FACS Diva software), analyzed using FlowJo X software, and plotted using the GraphPad Prism software. Spheroids alone were used to assess the percentage of apoptotic cells in normal conditions and were used to normalize the results obtained in presence of Vγ9Vδ2 T cells. For Vγ9Vδ2 T cell perforin and granzyme-B staining, $15x10^4$ expanded Vγ9Vδ2 T cells were co-cultured with one spheroid following the conditions described above. Vγ9Vδ2 T cells were resuspended and washed in PBS, strained over a 40 μM filter and stained for FACS for 20 min at 4°C in the dark. Antibodies used were FITC-conjugated anti-human TCRg/d (REA591, Miltenyi Biotec), BV421 anti- human CD3 (SK7, BD Biosciences) for extracellular staining and a viability marker (LIVE/DEAD Aqua, Life Technologies). After a Fixation/permeabilization for 20 at 4°C using Cytofix/Cytoperm kit (BD Biosciences) and washes in Permwash buffer (BD Bioscience), Vγ9Vδ2 T cells were stained intracellularly for 20 min at 4°C in the dark. Antibodies used were PE-conjugated anti-Human Perforin (δG9, BD Biosciences) and PECF594 conjugated anti-human Granzyme-B (GB11, BD Biosciences) for intra-cellular staining. Samples were assessed using FACS LSR2 (Becton Dickinson), analyzed using FlowJo X software, and plotted using the GraphPad Prism software.

Recombinant Vγ9Vδ2 TCR production and competitive binding assay

A recombinant Vγ9Vδ2 TCR (clone G115) (Allison et al., 2001) with a C-terminal Fc-tag on the Vγ9 chain was produced in CHO cells, then purified using protein A column chromatography followed by buffer-exchange into PBS, then conjugated to AF647 fluorochrome (Thermofisher) following manufacturer's instructions. In some experiments Vγ9Vδ2 TCR-Fc were biotinylated using protein labeling kit following manufacturer's instructions (Thermofisher). Biotinylated proteins were then tetramerized with streptavidin-APC (Biolegend) at 4:1 molar ratio by adding the streptavidin over 10 times intervals to maximize tetramer formation. Cells were incubated with human Fc Block (Miltenyi Biotec) and then saturated with anti-BTN2A1 mAbs or isotype control (10 μg/mL) for 1 hr at 4°C. Cells were then washed and stained with the indicated concentrations of recombinant Vγ9Vδ2 TCR-Fc-AF647 or tetrameric Vγ9Vδ2 TCR-Fc at 10 μg/ml for 1 additional hour. After new wash, AF647 mean fluorescence intensity (MFI) was assessed by flow cytometry. For ELISA assay, recombinant human BTN2A1-His protein (R&D Systems) was coated (1 μg/mL) overnight at 4°C in Maxisorb 96-well plates (Nunc). Wells were washed 3-times in PBS, then saturated for 2h at RT in PBS-BSA 5%, and for 1 h at RT with the indicated anti-BTN2A mAbs or mouse IgG1 (2 μg/mL). Wells were washed 3-times before incubation with the indicated concentrations of Vγ9Vδ2 TCR-Fc for 1 h at RT, and further 3 washes in PBS. Vγ9Vδ2 TCR-Fc binding was revealed with anti-human Fc-HRP (Thermofisher) with TMB substrate. For coating control, an anti-His-HRP (Biorad) was used.

Assessments of antibody affinity toward BTN2A1

Antibody affinity toward BTN2A1 protein was conducted at using Biolayer Interferometry (BLI) technology on Octet Red96 platform (Fortebio/PALL). Recombinant human BTN2A1-His protein was used as analytes, and anti-murine Fc AMC Sensors (Fortebio/PALL). For affinity assessments, the antibody of interest was diluted in kinetic Buffer (1X, ForteBio/PALL) and loaded on the sensor with a loading target level of around 1 nm. Experiments were conducted at +30°C under shaking conditions (1000 rpm). A standard 5 steps protocol was used: (i)loading step: capture of the antibody (ligand) on the sensors, (ii) equilibration step (Baseline) in kinetics buffer 10X, (iii) association step: dipping of sensors into the analyte, (iv) dissociation step: dipping of sensors into Kinetics Buffer 10X, and (v) regeneration. For the first run, the standard working concentration ranged from 200 nM to 3.125 nM with ½ dilution. When necessary, for the second run, working concentrations were adjusted (from 80 nM to 1.25 nM).

Epitope binning assays

Epitope binning assays were also conducted using the same BLI platform. All antibodies were diluted at a concentration of 10 μg/mL in Kinetic buffer (Fortebio/PALL) and were tested in a pairwise combinatorial manner against their target (BTN2A1). The « in-tandem » format was used for this assay. Before proceeding to binning experiment on BTN2A1 antigen, antigen binding to the antibodies was confirmed following the capture on HIS1K biosensors. For this kinetic screening, the loading of BTN2A1 on HIS1K (signal intensity: 1 nm) was followed by an association step for 3 min, then by a dissociation step of 3 min. Then, the antigen (BTN2A1-His) was immobilized on the biosensor (anti-Penta-His HIS1K biosensor #18-0038, Fortebio/PALL) and presented to the 2 competing antibodies in consecutive steps, as follows: baseline, antigen capture, baseline, saturating antibody, baseline, competing antibody, regeneration.

Quantitative PCR

Relative BTN3A1, BTN3A2 and BTN3A3 expression in HEK BTN2AKO cells and derived transductants were measured by quantitative real-time PCR using Fast Advanced TaqMan Master Mix and TaqMan™ probes (ThermoFisher Scientific), according to the manufacturer's protocol (ThermoFisher Scientific). TBP housekeeping gene was assessed for normalization. The qPCR was performed on QuantStudio 5 Real-Time PCR System (ThermoFisher Scientific) analyzed with QuantStudio 5 Real-Time PCR Software.

QUANTIFICATION AND STATISTICAL ANALYSIS

All statistics and graphs were calculated and depicted using GraphPad Prism 8.0.1 (GraphPad, Inc). See figure legends for details on statistical tests.